Role of Hydrogen in Industrial Decarbonization: A Case for Ammonia Industry in the United States

by

Abhishek Bose

B.Tech. & M.Tech in Chemical Engineering,
Indian Institute of Technology Kharagpur (2017)

Submitted to the Institute for Data, Systems, and Society
in partial fulfillment of the requirements for the degree of

Master of Science in Technology and Policy

at the

MASSACHUSETTS INSTITUTE OF TECHNOLOGY

September 2021

Author .....
Institute for Data, Systems, and Society
August 6, 2021

Certified by .....
Dharik Mallapragada
Research Scientist, MIT Energy Initiative
Thesis Supervisor

Accepted by .....
Noelle Eckley Selin
Professor, Institute for Data, Systems, and Society and Department of Earth, Atmospheric, and Planetary Sciences,
Director, Technology and Policy Program

Role of Hydrogen in Industrial Decarbonization: A Case for Ammonia Industry in the United States

by

Abhishek Bose

Submitted to the Institute for Data, Systems, and Society
on August 6, 2021, in partial fulfillment of the
requirements for the degree of
Master of Science in Technology and Policy

Abstract

Ammonia production contributes more than 1% of the global greenhouse gas emissions (GHG) while being used to serve a majority of the demand for nitrogen-containing fertilizer for agricultural use. While the predominant route for ammonia production today relies on natural gas as a source of energy and hydrogen for thermochemical Haber-Bosch (HB) synthesis, there is growing interest in electrically-driven routes that can reduce carbon-footprint of ammonia production, by relying on low-carbon electricity supply from variable renewable energy (VRE) sources. This electrically-driven ammonia route could not only serve existing uses for fertilizer production, but also be deployed to service energy needs for other end-use sectors where ammonia use is being contemplated (e.g. marine transport). Here, we evaluate the spatial variations in cost of the above electrically-driven ammonia process across the U.S. predominantly, for different scenarios of electricity supply as well as technology cost scenarios for 2030. Our approach goes beyond prior techno-economic assessments of electricity-driven ammonia production by explicitly accounting for variability in electricity supply and its implications on plant design, cost and emissions. This is achieved by using a least-cost integrated design and operations modeling framework that treats as variables the relative sizing of various units (e.g. electrolyzer, Air Separation Unit, renewables capacity), including deployment of alternative forms of on-site storage (battery energy storage, gaseous H_2 and liquid N_2). The overall mixed-integer linear programming (MILP) model is able to optimize for the minimum annualized cost of providing round-the-clock ammonia under the required system emission and flexibility constraints. We also evaluate dedicated grid connected VRE-based ammonia production for locations in close proximity to existing NH_3 production facilities and agricultural hubs in the US, to identify the cost-optimal VRE mix and storage requirements for future projections of grid scenarios in the US. Based on this framework, we are able to develop optimal sizing requirements for the facility in terms of VRE and capital investments in equipment to be able to sustain round-the-clock production. Our analysis shows that a standalone renewable ammonia production facility makes use of storage of intermediate products (N_2, H_2) in the production process

so as to be able to dispatch them during non-availability of renewable electricity. To meet the minimum power input necessary to operate the thermochemical HB process, electrochemical storage (e.g. Li-ion) is also needed. However, if the thermochemical HB process can be operated at less than nameplate feed flow rates, the need for Li-ion battery storage is minimized, allowing for more cost-effective production options.

Thesis Supervisor: Dharik Mallapragada
Title: Research Scientist, MIT Energy Initiative

Acknowledgments

The journey of being a part of the Technology and Policy Program at MIT has been enriching and challenging especially through the past year in the wake of the global pandemic. In this process of learning and growing as an individual, this thesis has been the core contribution of my work during the last two years. During this period, my interactions and learning opportunities through classes and industrial/research group partners have been of immense help to develop and hone the understanding of the topic while developing new insights.

In this process, I would like to firstly thank my advisor, Dr. Dharik Mallapragada who has guided me academically and professionally to firstly introduce me to the topic of Hydrogen driven decarbonization opportunities and then enabled to develop and answer the relevant research questions to ponder over. In addition, the contributions over the last year would not have been possible without the generous support from the MIT Energy Initiative including Dr. Emre Gencer and Dr. Guannan He who have worked and advised closely on the Hydrogen related work. I am grateful for the support of Dr. Karthish Manthiram and Dr. Nikifar Lazouski on their advice and help in working on the topic of industrial Ammonia decarbonization.

The experience of being at TPP would be definitely incomplete without the support of Barbara DeLaBarre who has enabled a seamless and most welcome transition and support during graduate school. This work would not have been possible without the wonderful support from my cohort, especially - Drake, Ragini, Cathy and Olivia to bounce ideas off of and for the smallest of logistical challenges to overcome. And lastly, I would like to thank my parents, late Grandfather and significant other to have been through this journey with me across continents but always there to be guiding and supporting me through the best and worst of times.

Contents

List of Figures

List of Tables

Chapter 1

Introduction

Global efforts on reducing greenhouse gas (GHG) emissions over the past decade have seen most success in the electric power sector, even as emissions from other sectors have seen modest declines or remained stagnant. For example, in the U.S., CO_2 emissions from the power sector declined by 26% during 2008-2018, while for the same period, transportation CO_2 emissions increased by 1.4% and industrial CO_2 emissions decreased by 9% [4]. Decarbonization pathways for these sectors often cite electrification as a potential pathway, which shifts the burden of emissions reduction from these sectors to the power sector, where continued growth of wind and solar generation is expected to further reduce the emissions intensity of electricity supply. While direct electrification of certain end uses is poised to grow rapidly (e.g. light-duty vehicles), it may be challenged in particular applications such as heavy-duty transport like shipping and aviation where high energy density requirements remain a key performance criterion. For these end uses, alternative energy carriers like hydrogen (H2) and by extension hydrogen-rich molecules like ammonia (NH_3) and other liquid fuels, produced using low-carbon pathways, remain an appealing prospect.

Ammonia currently forms the backbone of the fertilizer industry contributing to the manufacture of fertilizers either in the form of anhydrous ammonia or urea manufacturing or through nitrogen component in mixed fertilizers. Fertilizer use is projected to double by 2050 with a majority of the demand increase projected in developing nations in Asia and Africa - regions with relatively low natural gas sup-

ply and uncertain existing infrastructure. In addition, future uses of ammonia are being explored including transportation fuels, energy storage and transport opportunities.(Figure 1-1) These opportunities have resulted in the pertinent need to study electricity based ammonia production as a pathway to sustainable and decentralized ammonia production processes which can meet the need for existing as well as future low-carbon energy system uses.

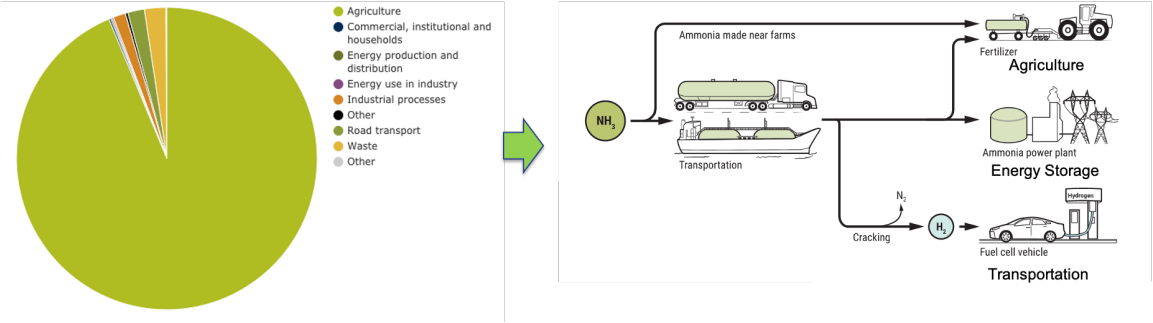

Figure 1-1: Major Uses of Ammonia by Sector : Current Uses (left)[1], potential uses (right)[2]

In a low-carbon energy system context, Ammonia offers some distinct advantages over other energy carriers, such as being carbon-free at point of use, increased volumetric energy density vs. compressed H_2, ease of storage and transport compared to liquid or gaseous H_2 and long-track record for safe handling at scale.[5, 6, 7] The predominant route for ammonia production relies on natural gas as a source of energy and hydrogen for thermochemical Haber-Bosch (H-B) synthesis, and is estimated to result in about 2.3 tonnes of CO_2 per tonne NH_3 produced. [8] The reliance on natural gas for ammonia production also implies that cost of ammonia is a key driver of the effective landed cost of the ammonia, ranging from USD 300-400/tonne depending on the swing in Natural Gas prices in the U.S. context [9], but potentially more open to price variations in other developing regions where natural gas cost is volatile, either due to supply or infrastructure limits. (e.g.: India fertilizer prices are expected to increase by 3.9% from 2017-2022)[10], Africa average ammonia prices range up to 700 USD/tonne [11, 12])

Declining costs of variable renewable energy (VRE) based electricity and elec-

trolyzers have raised interest in producing low-carbon H_2 via electrolysis, as well as its use in decarbonization of industrial ammonia production.[13, 14, 15, 16] This route is among the most technological mature process concepts for electrochemical ammonia production[17, 18, 19] and paves the way for emerging electrochemical ammonia production pathways that are modular and hence, amenable to deployment at smaller scales as compared to the conventional fossil-fuel driven process.[17, 20] As noted earlier, electrically-driven ammonia production is potentially appealing for many developing countries with relatively high natural gas costs, and where ammonia use for fertilizer is projected to grow rapidly over the next few decades.[21] Finally, the ease of handling and storage of liquid ammonia relative to hydrogen also opens up the potential for use of ammonia as a potential energy storage vector with relatively high energy density via Power-to-NH_3-Power cycles.[22].

Chapter 2

Overview of Existing Work on Green Ammonia Systems

Several recent studies have investigated the techno-economics of electrically driven ammonia productions via low temperature electrolytic hydrogen production coupled with thermochemical H-B synthesis. These studies tend to focus on one or more the following aspects: a) NH_3 costs in particular geographical region, ranging from the Middle East [23], Iceland [24], Germany [25], Chile [26], China [27] and India [28], b) alternate electricity supply, ranging from co-located VRE supply as part of islanded systems [29], to grid+contractual VRE supply via power purchase agreements [30], c) representation of ammonia production requirements and process operational constraints, which are included in varying detail by some studies [25, 31, 32] but overlooked in other cases[29, 33, 34, 35] and d) inclusion of alternative on-site storage technologies to manage temporal variability in electricity supply, either from the grid or on-site or contracted VRE sources[26, 30, 32]. Here, we note the salient contributions of some of these studies, while noting their differentiating aspects related to model fidelity (i.e. temporal resolution, demand and operational constraints), regional characteristics and level of decarbonization evaluated (see Table 2.1). Nayak-Luke et al. [29] evaluate the effect of intermittent renewable electricity on running a thermochemical Haber-Bosch process reactor with electrolytic H_2 supply. They model definite co-located PV and wind infrastructure mix ratios as electricity supply at a

single location while optimizing for the H-B system size that also accounts for the process flexibility. However, the authors do not model grid-based electricity supply or the full-spectrum of storage options to manage VRE variability. Banares-Alcantara et al.[36] evaluate the outcomes based on a localized islanded ammonia generation facility, but overlook the variability in VRE availability [29]. Morgan et al.[34] study offshore wind driven ammonia production in the United States (U.S.) context while incorporating intermediate storage for the physical ammonia process components but overlook the time and price variations in grid and wind farm power output and its impact on hourly process operations and overall cost. Osman et al.[32] develop a techno-economic model that incorporate the effects of variability in solar resource, the flexibility of the subsystems such as ASU, electrolyzers as well as an ASPEN based process model, to study design and operations of a renewable ammonia system in the middle east. However they overlook the role of grid integration which, as we discuss in later sections, may allow for lowering ammonia costs and eventually CO_2 emissions as well. On similar lines, Armijo et al. [37] focus on studying the potential for renewable ammonia production in Chile & Argentina through a temporally resolved optimization model and conclude that the combination of wind and solar resources for electricity supply can drive down costs by reducing the overall variability in energy supply. The authors also study the role of flexible H-B proces operation as a key driver for eventual reduction of costs. Schulte Beerbuhl et al [38] propose a more granular modelling approach to evaluate the non-linearities of the operations for optimal grid electricity scheduling and storage investment, which can be useful for grid load monitoring and planning. Related to this, Allman et al. [39] have focused on evaluating the effects of wind intermittency in developing an techno-economic optimization model which focuses on evaluating the impact of infrastructure costs for sub-units in the process including cost of Wind VRE, ASU, Electrolyzer and others for ammonia generation primarily focusing on the US upper Midwest. The authors also study the role of intermediate nitrogen and H_2 storage to ensure round-the-clock operation.

In this study, we extend the existing literature by performing a detailed spatial

and temporally resolved analysis of electrically driven ammonia production via the process of Figure 3-1 in the US context. Our analysis is based on modeling the least cost design and operation of the process while considering three key attributes influencing the overall process economics: a) temporal variability in electricity supply from grid and/or co-located VRE generation, b) detailed process related considerations, including relative operational inflexibility in thermochemical H-B synthesis as well economies of scale of investment in certain unit operations (e.g. Air separation unit) and c) use of alternate on-site storage options to manage temporal variability in energy inputs, including intermediate and electricity storage. We use the developed model to evaluate cost of electricity-based NH_3 supply for various regions in the continental United States under alternate technology cost assumptions, carbon policy and electricity supply scenarios (dedicated VRE or grid based, VRE+ grid). Finally,we use the model to explore the economic value of introducing limited operational flexibility in thermochemical H-B synthesis.

Table 2.1: Summary of recent work on electricity driven Ammonia production techno-economic modelling

Reference	VRE Sources Considered	Modelled Operations Variability?	Grid Connection?	HB Synthesis Loop Process Model?	Storage Options	HB Process Flexibility?	Region
Nayak Luke et al.[29]	PV, Wind	Yes	No	No	H_2 only	Yes	UK
Guerra et al.[26]	No	No	PPA	No	NH_3 only	No	Chile
Maia et al.[24]	Wind	No	No	No	NH_3 only	No	Iceland
Osman et al.[32]	PV, CSP	Yes	No	Yes	H_2, N_2, NH_3	No	UAE
Morgan et al.[34]	Wind	No	Yes	No	H_2, N_2, NH_3	No	USA
Beerbuhl et al.[38]	No	Yes	Yes	No	H_2 only	No	Germany
Allman et al.[39]	Wind	Yes	No	No	H_2, N_2, NH_3	No	USA
Nosherwani et al.[25]	Wind	Yes	No	Yes	H_2, N_2, NH_3	No	Brazil
Liang et al.[31]	-	-	-	Yes	-	Yes	Netherlands
Zhang et al.[40]	-	-	Yes	Yes	-	No	Italy
Current Work	PV, Wind	Yes	Yes	Yes	H_2, N_2, NH_3,Li-ion	Yes	USA

Chapter 3

Ammonia Techno-Economic Modelling Methodology

The integrated design and operations modeling framework used in this study and adapted from prior work [41] incorporates the the unique features influencing design and operations of industrial processes like ammonia production: a) round-the-clock operation to maximize capacity utilization, b) centralized production to maximize economies of scale of thermochemical processing and c) limited operational flexibility owing to large thermal inertia of units, and d) extensive heat and mass integration within the process. We formulate the design and operations assessment as a mixed integer linear program (MILP) with an objective function corresponding to the sum of the annualized investment (CAPEX) and operating (OPEX) cost of operating the ammonia production facility shown in Figure 3-1. This objective is minimized subject to a variety of operational and policy constraints that are enforced to model plant operations throughout the year on a hourly resolution, resulting in 8760 operational periods. The resulting MILP model is solved via Gurobi [42] run on a Xeon-g6 processor with 4 GB of ram across 32 cores on each compute node[43]. The average time to converge for each run ranges from 100-500seconds. The base system design parameters are shown in Table 3.1. Below, we describe the modeling of the various unit operations in the process along with a summary of the key cost and performance assumptions impacting their design and operations.

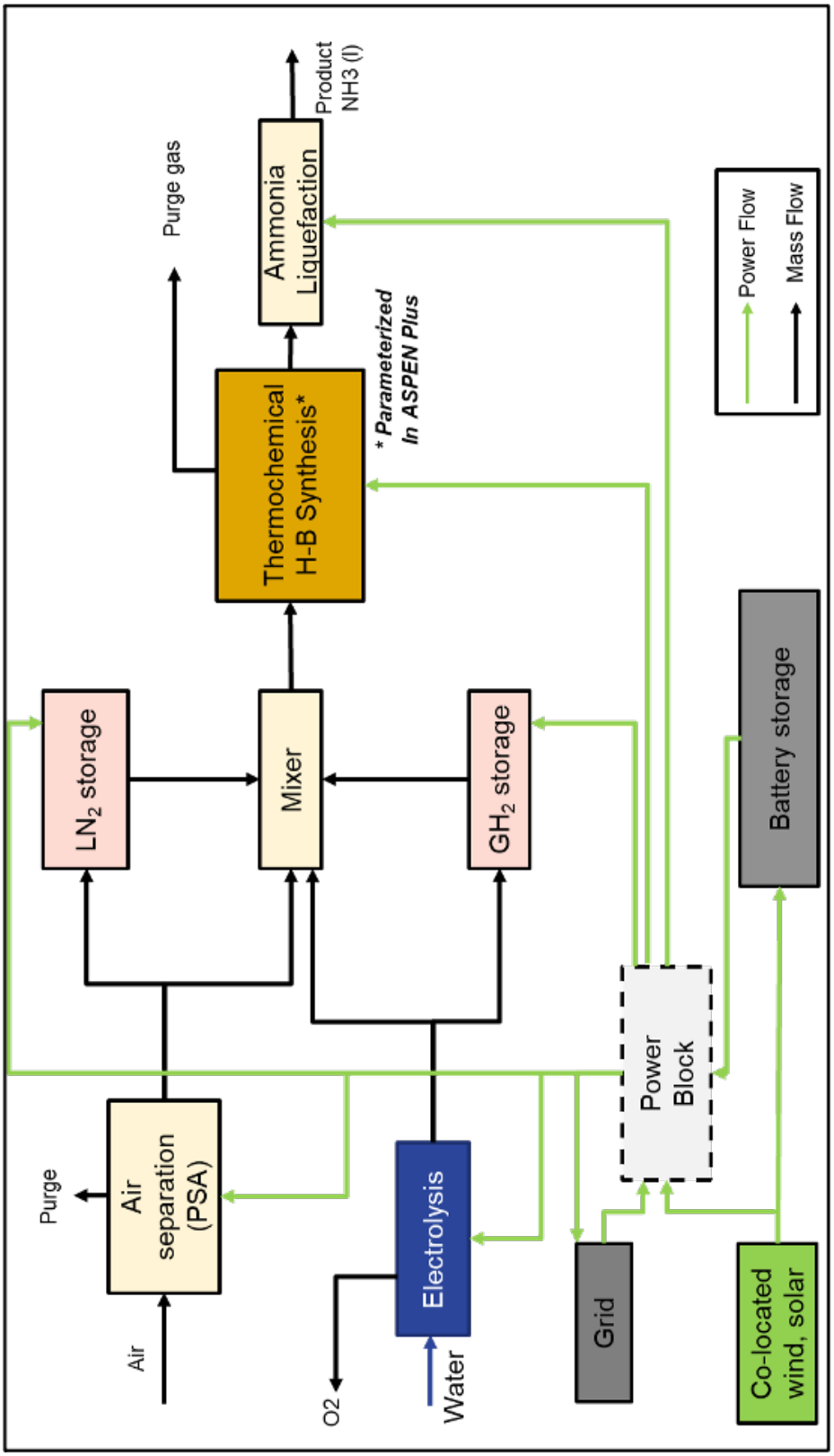

Figure 3-1: Electrolytic-H2 + Thermochemical HB Process Flow

Table 3.1: System Design Parameters for Electricity-Driven ammonia System

Parameter	Value	Units
Ammonia Production Capacity	250	$tonnes/day$
Plant minimum Down time	48	$hours$
CAPEX contingency Factor	21	%
Discount Rate	8	%
Weather Year	2011	
Cooling Water Use	1000	$tonnes/tonne NH_3$
Cooling Water Cost	0.0148	$\$/tonne$
Plant Annual Availability	95%	
Grid Interconnection Cost	0.03	$\$/Watt$

3.1 Electrolyzer

H_2 production via low-temperature electrolysis is modeled based on available cost and performance projections for proton exchange membrane (PEM) electrolyzers for 2030, that includes producing pressurized H_2 to 30 bar which could be stored and pressurized for H-B process requirements. The electrolyzer is considered to be fully flexible in terms of adjusting its power consumption from one hour to the next, which is consistent with flexibility of PEM systems. The electrolyzer lifetime is considered to be around 12 years based on the average stack replacement lifetime for the system. The model sizes the optimal electrolyzer capacity as well as enforces hourly operational constraints to track the power inflow into the system and produced H_2 stream flow rates to the storage and H-B unit (Eqn:4.10-4.13).

Table 3.2: Electrolyzer Cost Design Parameters. FOM = Fixed Operations & Maintenance.

Parameter	Value	Units	Reference
Operating Pressure	30	bar	
CAPEX	500	$\$/kW$	[8]
FOM cost	5	%	[44]
Specific Power	53	kWh/kg	[8]
Lifetime	20	$years$	

3.2 Storage

We model various forms of storage analogous to a common structure considering the role of energy and power in the system. The four possible storage types modeled include -

- Li-ion Battery Storage
- Gaseous Hydrogen (Above Ground Storage)
- Liquid Nitrogen Storage
- Liquid Ammonia Storage

The primary design variables for each storage technology include storage's energy or mass capacity, as well as maximum rate of power or mass charging and discharging the storage. These design variables are coupled with operational constraints that track storage inventory levels from one hour to the next, as well as adherence to the installed capacity limits. We consider availability of ammonia storage only in the case when the H-B process is flexible and in that case, consider two potential storage forms: a) pressurized liquid ammonia for small scale storage choice at 20 bar and, b) large scale cryogenic liquid ammonia storage at -33°C. The two choices are modelled via the same storage representation explained in equation 4.4-4.8.

Table 3.3: Storage Costs & Operational Parameters

	Energy CAPEX	Power CAPEX	FOM Energy	FOM Power	Energy Units	Power Units	Reference
Li-ion Battery	116000	101000	2987	2240	MWh	MW	[45]
H2 Storage	345000	1200000	3450	48000	tonne	tonne/hr	[46]
N2 Storage	1916	476000	19	19040	tonne	tonne/hr	[47]
NH3 Pressurized	5058	60	50	0	tonne	tonne/hr	[48]
NH3 Cooled Storage	719	60	7	0	tonne	tonne/hr	[48]
Units	*$/Energy Unit*	*$/Power Unit*	*$/Energy Unit*	*$/Power Unit*			

3.3 Nitrogen generation

Nitrogen (N_2) generation is modeled based on a pressure swing adsorption (PSA) unit, that is assumed to be adjust its output from one hour to the next without any limitations. PSA units tend to operate in a cyclical steady-state and this mode of operations allows for operational flexibility that can be leveraged in an electrically-driven ammonia production process.[49] The PSA is considered to produce N_2 which is then connected to a liquefaction set up for liquid Nitrogen storage.To account for the economies of scale in the PSA process, we model the capital cost of the system as a piecewise linear function of capacity using 5 piece-wise linear segments (see Equation 4.15-4.20). The PSA is modelled to produce output at 30 bar which is then split into two streams - directly flowing into the H-B synthesis loop or being liquefied for storage. The stored liquid N_2 is pumped into the H-B stream at the reactor pressure for further use. The primary design variable is the sizing of the PSA system which is decided based on the maximum production rate of N_2 desired for operating the HB synthesis loop.

3.4 Haber-Bosch (H-B) synthesis loop

The HB synthesis loop section is simulated in ASPEN plus based on the flowsheet shown in Figure 3-2, to consider the input of pure H_2 and N_2 streams from the up-stream production facilities modelled above. The H-B synthesis loop consists primarily of three sections: a) the compressor train to compress the input feed gas (mixture of H_2 and N_2) at 30 bar to 250 bar for the H-B reactor, b) the H-B reactor which is maintained at a temperature of 500°C with a heat recovery exchanger to recover waste heat from the output stream and c) finally a flash tank which separates and liquefies the output NH_3 in the system to produce liquid ammonia. For the optimization model, the H-B synthesis loop is treated as a black box with pre-defined process operating parameters related to power requirement, cooling water and other utilities are considered from the output of the system for modelling the operations of the HB

unit.

While the electrolysis and PSA generation systems are designed to be fully flexible to adjust their operation as per production needs and available power supply to the system, the H-B reactor (and by extension the synthesis loop) is inherently less flexible in nature with resulting constraints in ramp rates and operational flexibility. Currently deployed H-B synthesis facilities tend to run near constant output and we have incorporated this constraint in our modeling. At the same time, to understand the role of flexible systems and the impact on cost - we introduce two parameters to understand the nature of flexibility in the system: shutdown times and ramp rates. The shutdown time constraint is implemented in line with modelling scheme of Mallapragada et al.[41] considering a minimum down time of 48 hours for the H-B system.(Equation 4.21-4.26,4.31-4.32,4.2.2)

Table 3.4: Ammonia Synthesis Specific Parameters

Parameter	Value	Units	Reference
HB Synthesis Unit	3,734wh,400	*$/(tonne/hr)*	[50]
HB Unit Power Use	0.725	*MW/(tonne/hr)*	Appendix A
ASU CAPEX	150,000	*$/(tonne/hr)*	[36]
ASU Power Use	0.29	*MW/(tonne/hr)*	[36]

3.4.1 Thermochemical Ammonia Synthesis Loop Process Model

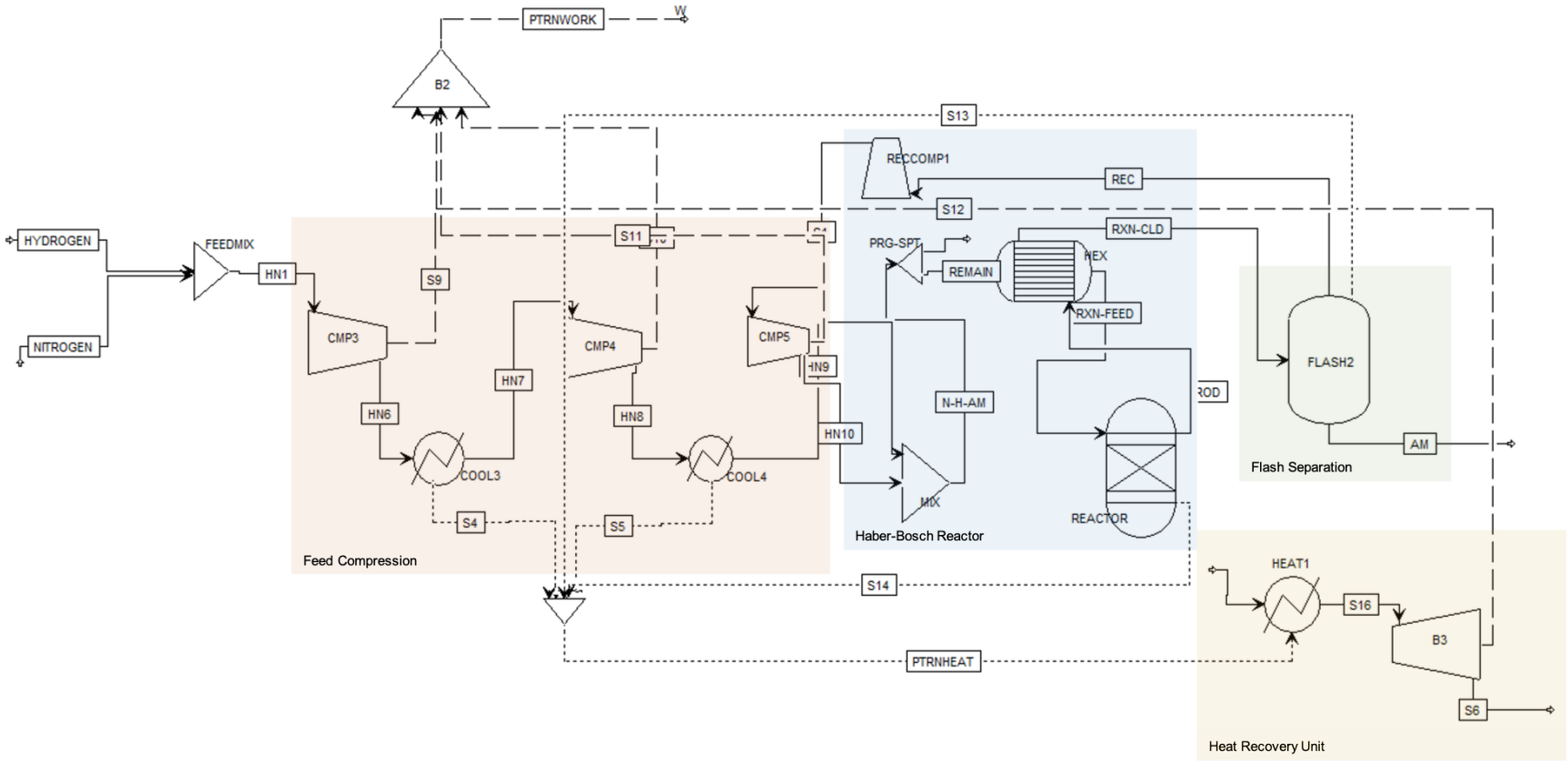

Figure 3-2: ASPEN Flowsheet for HB Synthesis Loop Process Model

3.5 Electricity supply

Electricity is the only energy input for the entire process and we consider the availability of VRE resources (solar (PV) and Wind) as well as connections to the grid (including grid interconnection + electricity supply costs and emissions) as a part of the set of available electricity sources in the system. The model takes inputs in the form of hourly VRE capacity factor data as well as electricity price time series (see Equation:4.1-4.3,4.37).

3.5.1 VRE resource modeling

Our analysis focuses on the extent of the contiguous continental U.S., where the overall landmass is divided into a grid of 1487 locations for extracting the relevant VRE availability information. The renewable energy resource availability curves is generated in line with Brown et al. [51] as described below. We consider renewable availability data for 2011 as a representative weather year for our analysis.

Hourly PV capacity factors (CF) are simulated using historical satellite-derived weather data from the National Solar Radiation Database (NSRDB)[52] as inputs to the open-source PVLIB model[53]. The native resolution of the NSRDB is 30min; modeled PV output is downsampled to hourly resolution using trapezoidal integration. All PV generators are assumed to employ horizontal single-axis tracking with a north-south axis of rotation (tracking from east to west throughout each day) and a DC-to-AC ratio of 1.3. Numerical assumptions (DC-to-AC ratio, system losses, temperature coefficient, etc.) are taken from Brown et al. 2020 [51] and generally match the assumptions used in the PVWatts model[54] and recent industry trends. PV capacity factors (CF) is simulated at an icosahedral mesh of sites spanning the continental U.S.(Figure 3-3(top))

Hourly wind CF is simulated using historical meteorological data from the NREL Wind Integration National Dataset Toolkit (WTK) [55, 56, 57, 58] and power curve data from commercial wind turbines assuming a 100m hub height. We simulated wind resource output based on the Gamesa G26/2500 turbine power curve for the purpose

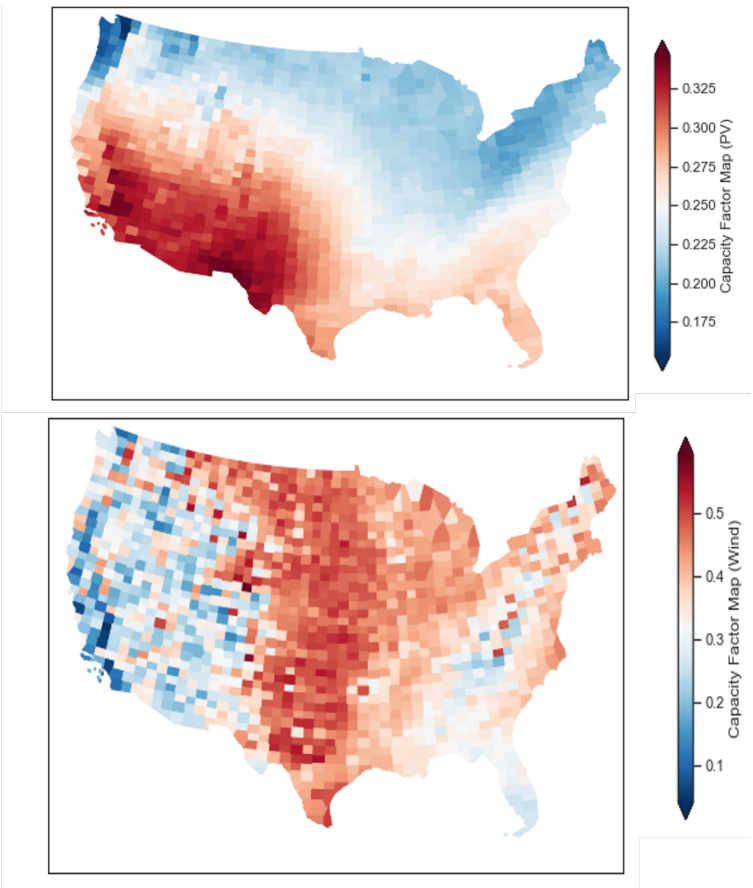

Figure 3-3: Average PV Capacity Factor (top), Average Wind Capacity Factor in continental US

of our study. A total of 42000 points in the continental U.S. was sampled which were then downsized to the 1487 points grid considered for our study by locating the points closest to the grid locations.(Figure 3-3 (bottom))

Table 3.5: VRE Resource Cost assumptions

Resource	CAPEX *$/kW*	FOM *%*	Lifetime *years*	Reference
PV	500	1	20	[45]
Wind	1200	2	20	[45]

3.5.2 Grid Electricity Input

To evaluate the effect of wholesale electricity price and CO_2 emissions intensity on ammonia production, we use electricity price profiles corresponding to 2030 available

from the 2020 standard scenarios grid modeling results for the U.S. [59]. Specifically, we use simulated 2030 electricity prices and marginal emission factors data from the above reference for each balancing area corresponding to the medium renewable penetration scenario. The spatial distribution in average CO_2 emissions intensity for the region under focus in our study is presented in Figure 3-4. (Map of corresponding average Locational Marginal Prices in Figure 3-5) We model an electricity based Ammonia synthesis system which interacts with the system boundary primarily in the form of electricity inputs from the grid or VRE and in the form of outputs of liquid ammonia. While there is no emission from the considered system boundary - an important facet of this model is to account for the associated CO_2 emissions of the grid electricity supply in the produced ammonia, which allows for holistic assessment of shifting from natural gas to electricity driven processes. Therefore, the hourly electricity requirement from the grid is tracked and the corresponding marginal CO_2 emissions intensity of the supplied grid electricity at each time period is incorporated in computing the emissions intensity of ammonia production.[1]. As discussed in the results, this representation also allows for exploring trade-offs between grid supply vs. co-located VRE supply under various CO_2 policy scenarios.

[1]Marginal emission factors are modelled in place of average emissions to account for the hourly variability in emissions from the grid and operational changes resulting from VRE penetration of the grid - see Thind et al. [60] for further discussion

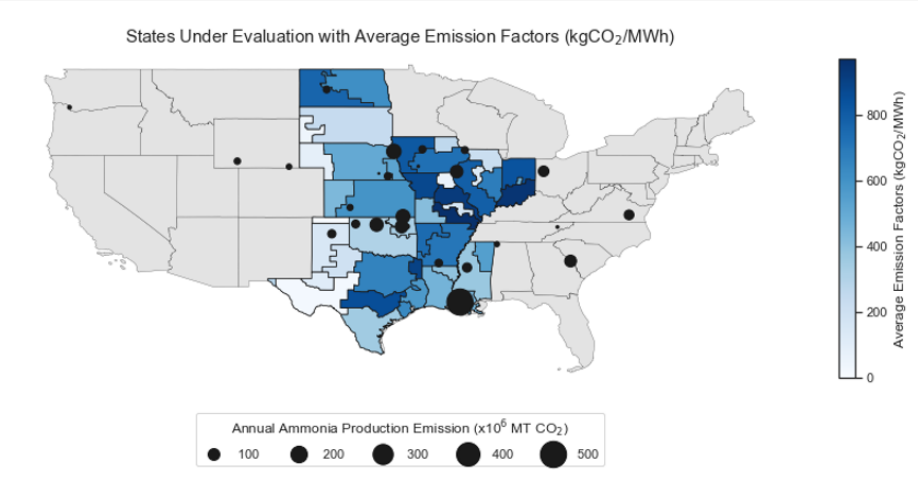

Figure 3-4: Average Emission Factor Map under NREL Cambium 2030 scenario for focus area of study in continental USA (Current top 20 Ammonia production facilities shown for reference locations[3])

2

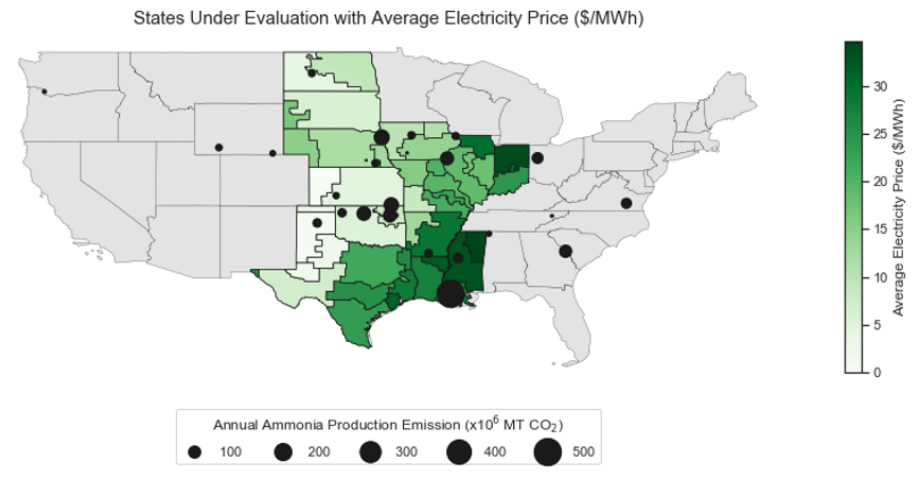

Figure 3-5: Average Electricity Price map under NREL Cambium 2030 scenario for focus area of study in continental USA (Current top 20 Ammonia production facilities shown for reference locations [3])

Chapter 4

Ammonia Techno-economics Model Formulation

Nomenclature

Sets

s	Set of Air Separation Unit CAPEX intervals	
i	System Components: [VRE,Stor,Ely,ASU,HB,Flash]	
j	Renewable Energy (VRE) types - 1:PV, 2:Wind	
k	Storage Types - 1:Li-ion, 2 - $H_2, 3 - N_2, 4 - NH_3$	
s	ASU Piecewise Regimes	
t	Time Index (Time Index denoted in parenthesis)	

Parameters

η_i	Specific Electricity Consumption for component i	$MW/FlowRate$
$\eta_S tor$	Efficiency of Li-Ion Battery Storage	
$CapacityLB_{ASU_s}$	Lower bounds for ASU Installed Capacity	$tonnes/hr$
$CapacityUB_{ASU_s}$	Upper bounds for ASU Installed Capacity	$tonnes/hr$
CCF_i	Capital Charge Factor to Annualize CAPEX	
CO_2Price	Carbon price scenario under evaluation	$\$/kgCO_2$
$ElecPrice$	Locational Marginal prices of energy	$\$/MWh$
$flexrange$	Maximum allowable turndown ratio for HB Synthesis Loop	

FOM_i	Yearly Fixed OM Cost	$\$/year$
$MaxNH3HeatDuty$	Maximum heat duty to be removed from the NH3 liquefaction loop based on design capacty of the system	MJ
$MEF(t)$	Marginal Emissions from each unit of power drawn from the grid at time t	$kgCO_2/MWh$
$minHBavail$	% of hours HB unit is available	
$minPlantavail$	% of hours overall Plant is available	
$minTHBcf$	Minimum Ratio of HB Unit Output to Capacity	
$NH3DesignFlowRate$	Design Capacity for overall plant (hourly demand)	$tonnes/hr$
$pCF_j(t)$	Renewable Capacity Factor for VRE of type j at time t	
$PowtoFlash$	Power input to flash system for $NH_3 liquefaction$	MW
$UnitCAPEX_i$	Capital Investment per unit of installed capacity for technology i	$\$/CapacityUnit$
$UnitCAPEXLB_{ASU_s}$	Lower bounds for ASU CAPEX	\$
$UnitCAPEXUB_{ASU_s}$	Upper bounds for ASU CAPEX	\$

Variables

$ElyCap$	Installed Electrolyzer Capacity	MW
$GridtoPow(t)$	Power drawn from the grid at time t	MW
$H2flow(t)$	H_2 produced from electrolyzer at time t	$tonnes/hr$
$H2flowProd(t)$	H_2 flow rate to NH_3 synthesis loop from electrolyzer	$tonnes/hr$
$H2Total(t)$	Total flow rate of H_2 into the NH_3 synthesis loop	$tonnes/hr$
$N2flow(t)$	N_2 produced from ASU at time t	$tonnes/hr$

$N2flowProd(t)$	N_2 flow rate to NH_3 synthesis loop from ASU	$tonnes/hr$
$N2Total(t)$	Total flow rate of N_2 into the NH_3 synthesis loop	$tonnes/hr$
$N2Total(t)$	Total flow rate of NH3 to output including storage discharge	$tonnes/hr$
$NH3flow(t)$	NH3 produced from HB loop at time t	$tonnes/hr$
$NH3flowProd(t)$	NH3 flow rate to output HB loop	$tonnes/hr$
$PowtoASU$	Power flow to Air Separation Unit at time t	MW
$PowtoEly(t)$	Power flow to electrolyzer at time t	MW
$PowtoHB$	Power flow to HB Synthesis Loop	MW
$PowtoStor_k(t)$	Power flow to Storage technology of type k at time t	MW
$RetoPow_j(t)$	Power supplied from VRE of type j at time t	MW
$SoC_k(t)$	State of Charge (Stored Energy Level for storage technology of type k at time t	$EnergyUnits$
$StCharge_k(t)$	Storage Charge input at time t for storage of type k	$tonnes/hr$
$StDischarge_k(t)$	Storage Discharge output at time t for storage of type k	$tonnes/hr$
$StorCap_k$	Installed Storage Capacity of type k	$EnergyUnits$
$StorPowCap_k$	Storage Power Capacity of type k	$PowerUnit$
$THBInstalled$	Installed Capacity of HB Synthesis Loop	$tonnes/hr$
$vCommit(t)$	Binary Commitment variable tracking on/off state for entire Ammonia production facility	
$VRECap_j$	Installed VRE Capacity of type j	MW
$vTHBCommit(t)$	Binary Commitment variable tracking on/off state of HB synthesis loop production	

w_s	Binary Index of chosen ASU Capacity Interval	
x_s	Fractional capacity increase from lower bound of interval x	

Expressions

$CAPEX_i$	Total CAPEX for Installed Technology i	\$
$OPEX(t)$	Total operational expenses at time t	\$
$OPEXEmisson$	Emissions Cost to consider effect of carbon price	\$
$PowerConsumption(t)$	Total Power Consumed by the NH_3 production facility at time t	MW
$PowerSupply(t)$	Total Power supplied to the unit on time t	MW

4.1 Objective Function

$$Minimize : \sum_i CAPEX_i * CCF_i + \sum_t OPEX(t) + \sum_i FOM_i$$

i ϵ System Components

t ϵ Number of time periods in a year

4.2 System Components

Renewable Energy Capacity(VRE)

$$CAPEX_{VRE} = \sum_i (VRECap_j * UnitCAPEX_{VRE_j}) \tag{4.1}$$

$$OPEX_{VRE} = \sum_i FOM_{VRE_j} * VRECap_j \tag{4.2}$$

$$PowerBalance : RetoPow(t) <= \sum VReCap_j * pCF_j(t) \tag{4.3}$$

Storage (Stor)

Energy Storage is modelled in the form four possible storage intermediates in the Ammonia production process -

- Li-ion Battery Storage
- Gaseous Hydrogen (Above Ground Storage)
- Liquid Nitrogen Storage
- Liquid Ammonia Storage

The primary component being modelled are the energy capacity of the storage technology and the cost of introducing the rate of charging (storing) and discharging (dispatch) limits on the system. For both batteries and physical storage medium - the same analogous parameters are considered albeit in different physical units.

$$CAPEX_{Stor} = \sum_{k} (UnitCAPEX_{Stor_k} * StorCap_k) \tag{4.4}$$

$$OPEX_{Stor} = \sum_{k} (FOM_{Stor_k} * StorCap_k) \tag{4.5}$$

Energy Balance :

$$k = 1 : SoC_1(t) = SoC_1(t-1) + PowtoStor_1(t) * \eta_{Stor} \tag{4.6}$$

$$k > 1 : SoC_k(t) = SoC_i(t-1) + StCharge_k(t) \tag{4.7}$$

Power Balance :

$$StorPowCap_k >= \eta_{Stor} * StCharge_k(t) \tag{4.8}$$

Electrolysis (Ely)

$$CAPEX_{Ely} = UnitCAPEX_{Ely} * ElyCap \tag{4.9}$$

$$OPEX_{Ely} = FOM_{Ely} * ElyCap \tag{4.10}$$

Power Balance :

$$PowtoEly(t) * \eta_{Ely} = H2flow(t) \tag{4.11}$$

Mass Balance :

$$H2flow(t) = H2flowProd(t) + StCharge_2(t) \tag{4.12}$$

$$H2flowProd(t) + StDischarge_2(t) = H2Total(t) \tag{4.13}$$

Air Separation Unit (ASU)

The Air Separation Unit CAPEX is modelled as a piecewise linear function with decreasing unit CAPEX with higher installed capacity to make use of the increased economies of scale. This is modelled as a set of unit CAPEX costs based on individual range of installed capacities.

$$CAPEX_{ASU} = \sum_s ((w * UnitCAPEXUB_{ASU_s} + x(UnitCAPEXUB_{ASU_s} - UnitCAPEXLB_{ASU_s})) \tag{4.14}$$

$$Capacity_{ASU} = \sum_s ((w * CapacityUB_{ASU_s} + x(CapacityUB_{ASU_s} - CapacityLB_{ASU_s})) \tag{4.15}$$

$$x_s < w_s \tag{4.16}$$

$$\sum_s w = 1 \tag{4.17}$$

$$PowtoASU(t) = \eta_{ASU} * N2flow(t) \tag{4.18}$$

$$N2flow(t) = N2flowProd(t) + StCharge_3(t) \tag{4.19}$$

$$N2flowProd(t) + StDischarge_4(t) = N2Total(t) \tag{4.20}$$

4.2.1 Thermochemical Haber-Bosch Unit (HB)

$$CAPEX_{HB} = UnitCAPEX_{HB} * THBInstalled \tag{4.21}$$

$$OPEX_{HB} = FOM_{HB} * THBInstalled \tag{4.22}$$

$$PowtoHB(t) = \eta_{HB} * NH3flow(t) \tag{4.23}$$

$$NH3flow(t) = NH3flowProd(t) + StCharge_4(t) \tag{4.24}$$

$$NH3flow(t) = N2Total(t) + H2Total(t) \tag{4.25}$$

$$N2Total(t) * 3 = H2Total(t) * 14 \tag{4.26}$$

$$NH3Total(t) = NH3flowProd(t) + StDischarge_4(t) \tag{4.27}$$

$$\tag{4.28}$$

Flash Unit (Flash)

The flash unit is considered as a refrigeration system which is designed to be handle the maximum outflow from the HB unit. The system CAPEX is rated in terms of $ per unit of heat to be removed from the system per unit time (MW). The power requirement for the system is considered as a function of the heat duty and the coefficient of performance for the refrigeration system

$$CAPEX_{Flash} = UnitCAPEX_{Flash} * MaxNH3HeatDuty \tag{4.29}$$

$$OPEX_{Flash} = FOM_{Flash} * MaxNH3HeatDuty \tag{4.30}$$

$$MaxNH3HeatDuty = Max(NH3flow(t)) * \eta_{Flash} \tag{4.31}$$

Power Balance:

$$PowtoFlash(t) = NH3flow(t) * \eta_{Flash} \tag{4.32}$$

4.2.2 Operational Cost Components

Emission Components

$$OPEXEmission(t) = GridtoPow(t) * MEF(t) * CO_2Price \tag{4.33}$$

System Power Balance

$$PowerSupply(t) = \sum_i (RetoPow_i(t) + \tag{4.34}$$
$$GridtoPow(t) + StDischarge_1(t))$$

$$PowerConsumption(t) = PowtoStor(t) + PowtoEly(t) \tag{4.35}$$
$$+PowtoASU(t) + PowtoHB(t) + PowtoFlash(t)$$

$$PowerSupply(t) = PowerConsumption(t) \tag{4.36}$$

OPEX Calculation

$$OPEX(t) = GridtoPow(t) * ElecPrice(t) + OPEXEmission(t) \tag{4.37}$$

Plant Operational Constraint Setup

The HB unit in the plant is considered to be inflexible in terms of the level to witch the plant can be turned up or down during operations. Similarly, to account for realistic operations for the system - a minimum down time constraint is enforced to ensure the process unit operations cannot switch between on/off state rapidly as would be expected in a realistic situation.

For each time period of operations, the activation of the system is tracked using binary variables (commitment variables) which signify the constraints to the production system. For reference - the overall production facility is considered to have two sections whose commitment is being tracked - the HB unit (THB) and the overall Ammonia plant (Plant).

Commitment Constraints:

$$THB : \sum_{t} vTHBCommit(t) >= minHBavail * 8760 \tag{4.38}$$

$$Plant : \sum_{t} vCommit(t) >= minPlantavail * 8760 \tag{4.39}$$

$$\tag{4.40}$$

Production Constraints:

$$THB : NH3flow(t) <= THBInstalled * minTHBcf * vTHBCommit(t) \tag{4.41}$$

$$Plant : NH3Total(t) = NH3DesignFlowRate * vCommit(t) \tag{4.42}$$

Flexibility Constraints:

$$NH3Flow(t) - NH3Flow(t-1) <= |flexrange * THBInstalled| \tag{4.43}$$

Chapter 5

Results & Discussion

5.1 Operational Dynamics of electricity driven ammonia production

We highlight the functionalities of the developed integrated design and operations model by discussing the model outcomes for two locations in the United States - first (A) Amarillo, TX and second (B) Greenfield, IN - based on the above-mentioned 2030 technology cost assumptions and under scenarios with and without use of 2030 grid electricity conditions. 2020-21 cost of natural gas based ammonia is around 0.4 USD/kg[61], while the levelized cost of ammonia (LCOA) of the grid only case is 0.5-0.6 USD/kg and the completely VRE driven case (VRE only)) is between 1 & 1.2 USD/kg at 2030 cost scenarios for the locations being evaluated (Figure 5-1). Based on simulated 2030 electricity prices and marginal emissions factors for the two locations, grid-electricity derived ammonia production has a positive abatement cost of 52 $/tonne CO2 (TX) and corresponds to 84% CO_2 emissions reduction in Amarillo, TX, while it has a negative abatement cost (-35 $/tonne CO_2) and leads to 176% (IN) greater CO_2 emissions Greenfield, IN. [1] Thus, while it is possible to realize 84% CO_2

[1]Cost of Carbon Abatement = $(LCOA_{Process} - LCOA_{incumbent})/(CO_2Intensity_{incumbent} - CO_2Intensity_{Process})$
We consider the difference in process emissions of the electricity driven and natural gas based incumbent technology for production of ammonia while upstream emissions are ignored for the purpose of this comparison. Inclusion of upstream emissions would provide values of abatement cost event

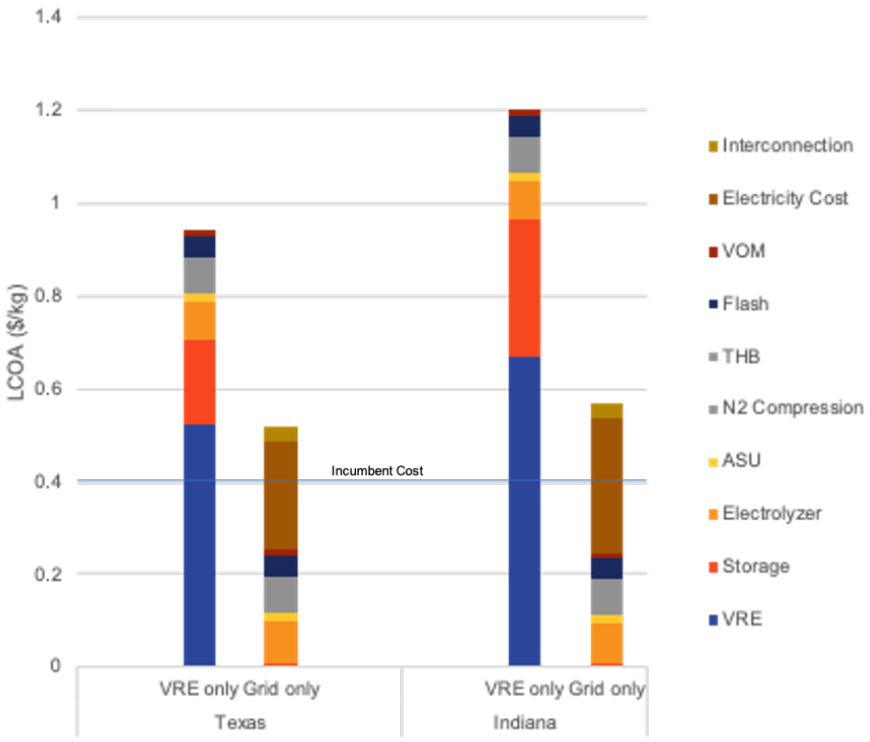

Figure 5-1: LCOA Comparison for VRE & Grid driven Ammonia production for sample locations in West Texas(Amarillo, TX) and Greensburg, IN for 2030 grid electricity price scenario

emission intensity reduction at a location with a low-emissions intensity grid (average grid emissions intensity at Amarillo, TX = 190 kgCO_2/MWh), connecting to a high emission grid (average grid emissions intensity at Greenfield, IN = 865 kgCO_2/MWh) results in higher specific emissions from each unit of produced ammonia and becomes a counter-productive solution in this case. This phenomenon is evaluated more closely for the case of continental USA in the following sections. 100% process CO_2 emissions is achievable at the two locations with a CO_2 abatement costs of 200 \$/tonne CO_2 and 297 \$/tonne CO_2 based on dedicated VRE electricity supply for the locations in TX and IN, respectively.

In addition to the levelized cost comparisons for these scenarios, the developed model provides detailed information of the investment requirements for each of the components in the facility (Figure 5-3) as well as the temporal dynamics of the system

lower than quoted in this study

operation in response to electricity supply variability. We simulate the operations of the facility to run at constant production flow rate, which results in a constant baseline power input for operating running the H-B synthesis loop as well as constant flow of the reactants into the H-B synthesis loop. Figure 5-2 highlights the temporal dynamics of the facility operation at the Texas location based on dedicated VRE supply and no grid access, where we see how operations are managed for low VRE availability periods (hours 25-65). Due to lower power availability, majority of energy intensive and flexible processes (H_2 generation through electrolyzer and ASU are turned down/off(Figure 5-2(a)) while discharging from the physical storage technologies.(Figure 5-2 (b,c) . The physical storage modes provide additional buffer capacity in order to bypass the energy requirement in the times of low resource availability or high electricity prices. Without grid connection, Li-ion battery storage is the only feasible option to provide the baseline power requirement for the base H-B synthesis loop during low VRE availability periods and contributes a 5-7% of total ammonia cost in both Texas and Indiana locations. Because of the availability of other types of cheaper storage, Li-ion storage is not used for managing the seasonal variations in the availability of VRE electricity.

$$LCOA = Annualized(CAPEX + OPEX)/YearlyNH_3Production$$

5.2 Estimated costs for dedicated VRE-based Ammonia Production in the United States

We evaluate the outcomes for both standalone solar(PV) and onshore wind driven ammonia production for continental U.S., and find that the resulting LCOA distributions largely follow spatial patterns in VRE resource availability owing to the dominant role of VRE capex in LCOA (results for PV only based facility configurations are described in Figure 5-5). For PV only systems, the key areas which provide the lowest LCOA are in the southwest of the United States. These regions, however, the lack of existing agricultural demand for ammonia (As inferred by location of ex-

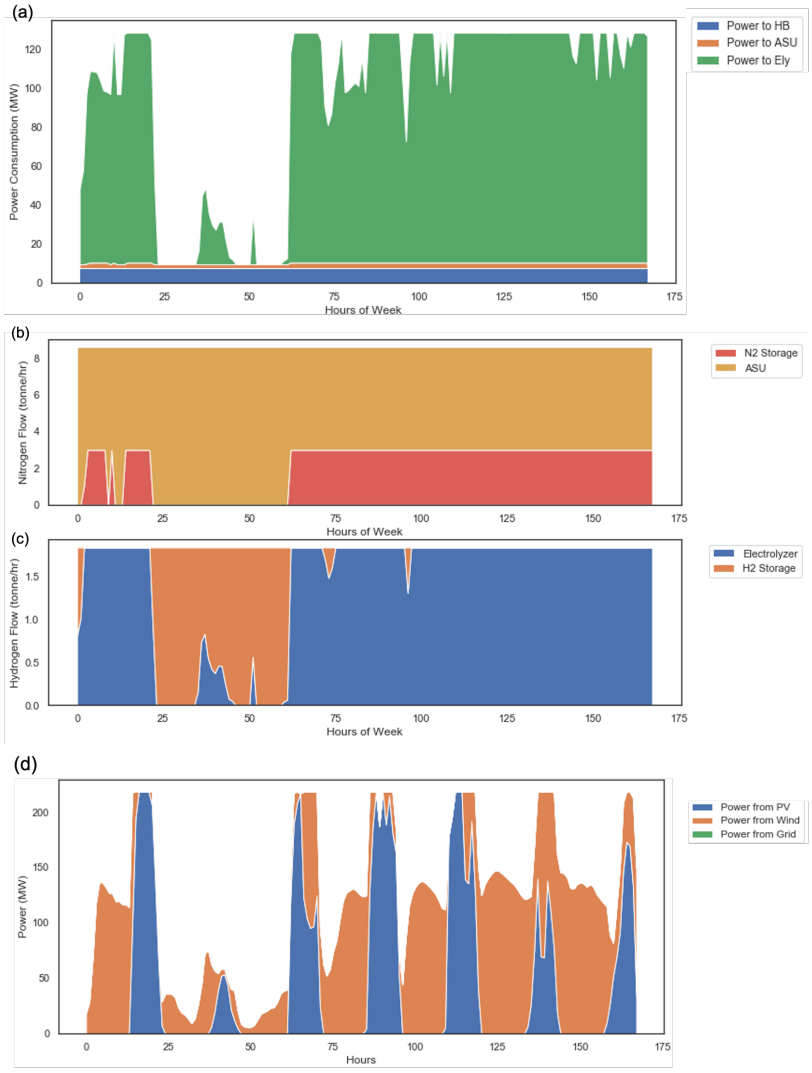

Figure 5-2: (a) Power Consumption Dynamics for a representative week (b)Nitrogen (c)Hydrogen flow dispatch from production technology and storage for input to HB synthesis loop (d) Power Supply profile from VRE technologies

isting ammonia production facilities), which might limit their short-term deployment value. For the emerging uses of ammonia as an energy carrier/fuel, these regions provide potential scope for generation to serve to demand centers such as California or the Gulf of Mexico region. In case of wind-driven ammonia production, the lowest cost regions better align with existing ammonia consumption regions, primarily the U.S Midwest, as shown in Figure 5-6. The costs of wind driven ammonia across the U.S. ranges from 1-12 USD/kg with about 92% of locations with a cost of less than 4 USD/kg (more than 10x the cost of current fossil fuel driven ammonia production)

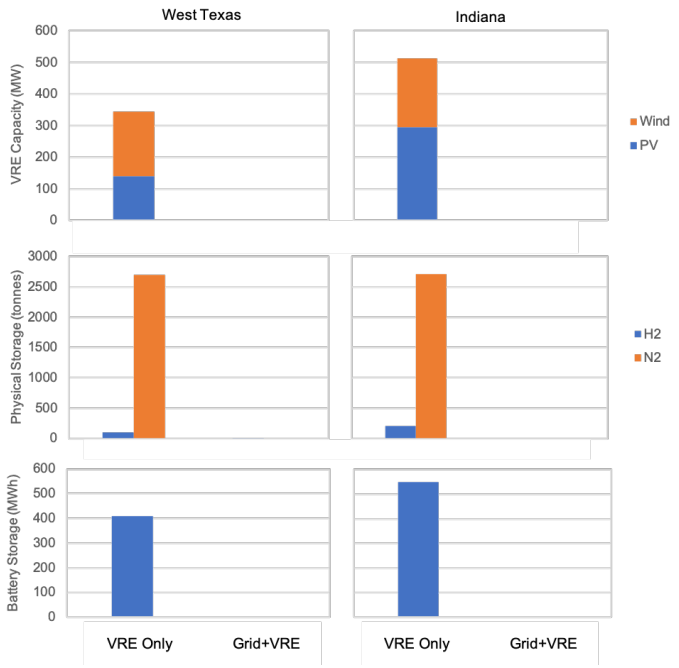

Figure 5-3: Investment Decisions for VRE and grid based Ammonia production for a sample location in West Texas(left) and Indiana(right)

The Midwest region currently accounts for most of the demand for fertilizers and collectively accounts for more than 90% of the ammonia producing facilities in the country (Figure 3-4). This provides for the potential for localized green Ammonia production through electrolytic Hydrogen coupled with co-located wind farms.

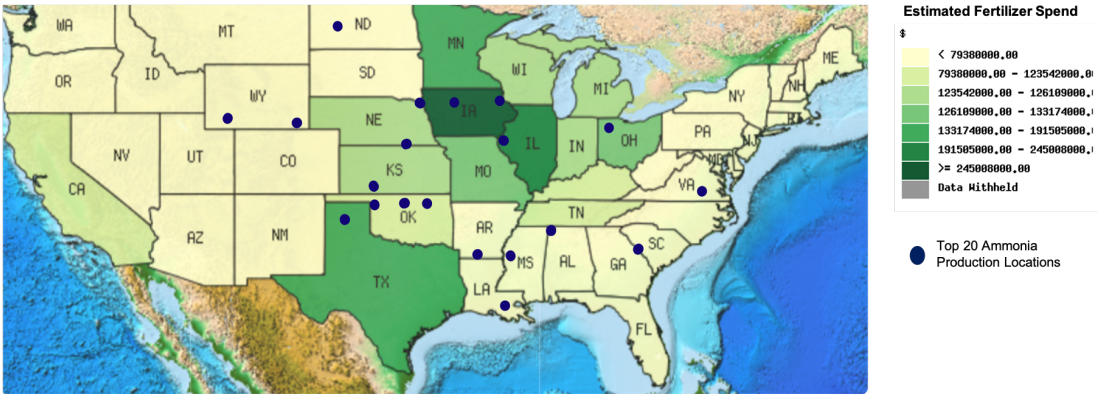

Figure 5-4: USA Fertilizer Consumption by State

Figure 5-5,5-6,5-7(a) highlights the spatial distribution in costs for dedicated VRE-based ammonia production across the continental U.S. where allow for both wind and

solar PV capacity to be deployed. Not surprisingly, allow for PV and wind resources to be used jointly results in lowering the cost of dedicated VRE-based Ammonia production to below 1 USD/kg levels for 12% of locations in the continental US paving the way for even further lowering the cost to produce the Ammonia from renewable electricity.

Combined renewable resource driven production provides the opportunity to access cheaper renewable ammonia in regions which may be able to utilize Ammonia in other forms of use such as a carrier for Hydrogen, liquid fuels among others. Especially, with newer use cases of Ammonia being explored such as maritime fuels, Hydrogen Energy storage - this would allow low cost Ammonia production in regions beyond the traditional agricultural and fossil fuel production regions.

Having an additional VRE source allows to reduce the need for daily storage requirements for the on-site production facility. While the base load of electricity to run the inflexible HB synthesis loop is balanced with a Li-ion battery, the battery capacity required reduces by on an average 10% for the sub-1USD/kg NH_3 regions identified in 5-7. The contribution to the electricity supply capacity is based on a majority of the contribution from the primary VRE resource in the region : for example, the Midwest region of United states is based on a major contribution from installed wind capacity - while buffered to a maximum around 40% of the capacity by PV installation. (Refer : Figure 5-8)

5.3 Carbon footprint and cost impacts of ammonia production using grid electricity

The above analysis indicates that while dedicated VRE based ammonia production can achieve full decarbonization, it is estimated to be more expensive than reliance on grid electricity based supply even with 2030 technology cost assumptions. Moreover, as the CO_2 emissions intensity of the electric grid is anticipated to decrease over time due to increasing VRE penetration, the relative CO_2 emissions benefits of pursuing

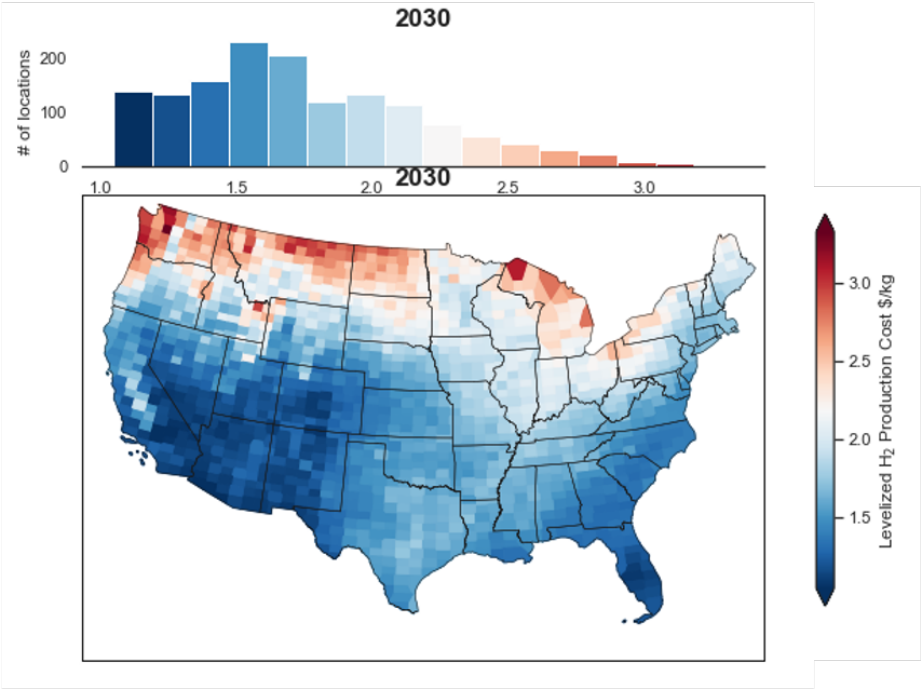

Figure 5-5: Levelized cost of Ammonia Map for PV driven Electrolytic Ammonia production

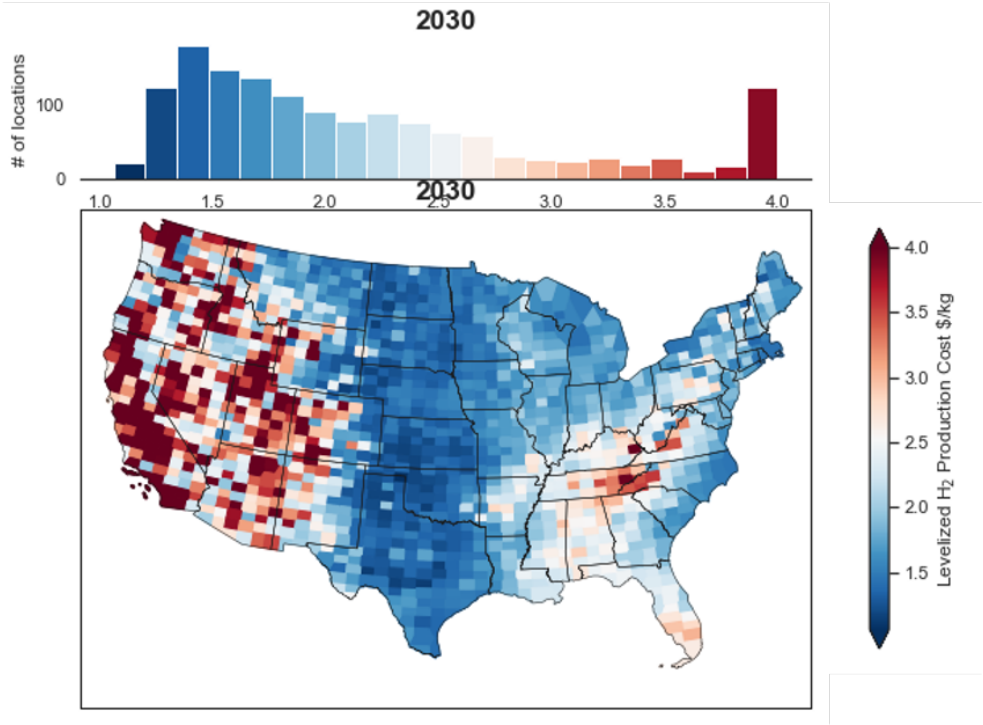

Figure 5-6: Levelized cost of Ammonia Map for Wind driven Electrolytic Ammonia production

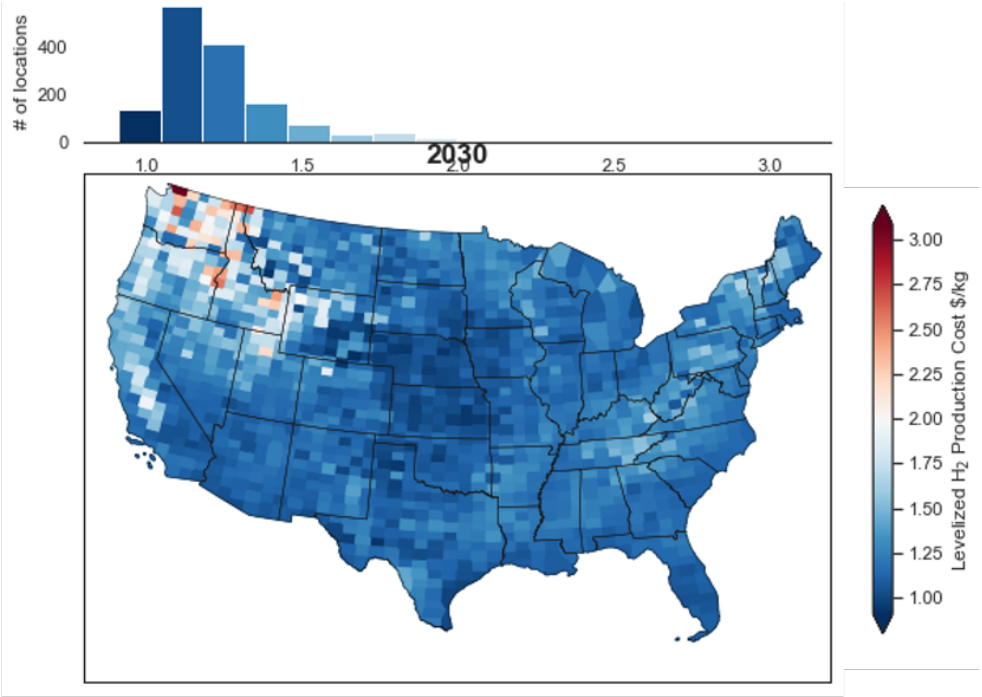

Figure 5-7: Levelized cost of Ammonia Map for PV+Wind driven Electrolytic Ammonia production

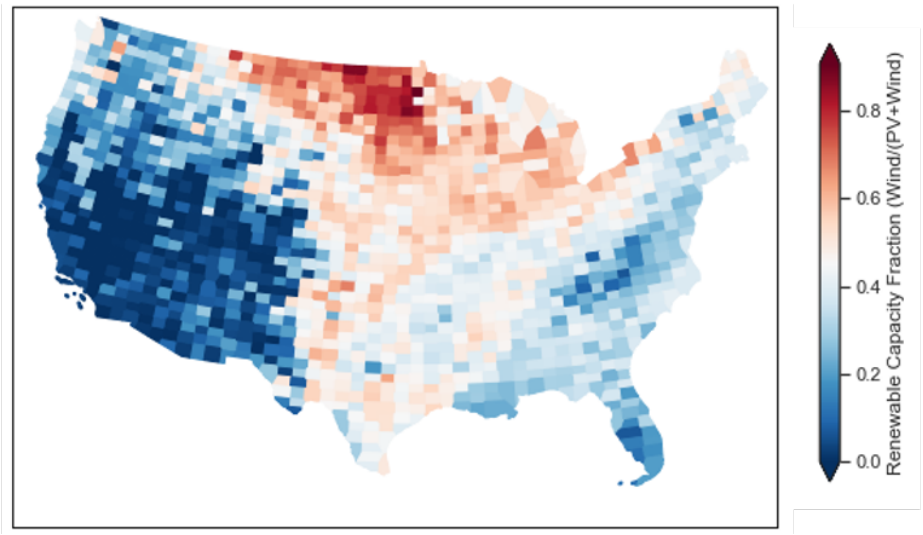

Figure 5-8: Ratio of Wind to total VRE Installed Capacity for combined Wind + PV deployment scenario

dedicated dedicated VRE electricity supply vs. grid electricity use are likely to diminish while the cost differences will remain. To understand this trade-off further, we explore the LCOA and process design outcomes for ammonia production using

grid+VRE electricity supply under various CO_2 price scenarios. As identified in the previous section, the key demand and supply hubs for ammonia currently are in the Midwestern states and Texas, and therefore we focus this part of our analysis on this region. We evaluate model outcomes for this region under the four carbon policy scenarios: no policy, low CO_2 price (10 USD/tonne CO_2), medium (50 USD/tonne CO_2) and high CO_2 price scenario (100 USD/tonne CO_2). The model is allowed to choose from all potential energy sources including VRE and grid electricity while calculating the LCOA and the CO_2 emissions intensity of produced ammonia. For the analysis,we consider model the grid in 2030 as per the standard scenario projections from NREL for price and marginal emissions for the system.

The results for the LCOA and CO_2 emissions intensities are shown in Figure 5-9 which focuses on depicting the variations in LCOA and CO_2 emissions intensity of ammonia production under the various policy scenarios. The spatial distribution of the LCOA map highlights that a under the no policy scenario, grid connectivity leads to relatively small spatial differences in LCOA outcomes but significant spatial variations in CO_2 emissions intensity. For example, ammonia production in Texas, North & South Dakota and Nebraska is estimated to 60-80% lower carbon intensity than ammonia production in Indiana or Illinois. A 50 USD/tonne CO_2 policy leads to greater role for VRE generation in electricity supply for ammonia production and leads to more spatially uniform CO_2 emissions intensity outcomes. Moreover, under this scenario, the CO_2 emissions intensity of ammonia production across most of the evaluated locations is below that of natural gas-based ammonia production. This is achieved by deploying more on-site VRE capacity at previously high-emission locations that can displace electricity use during high marginal emission intensity time periods of the day.

In general, increasing VRE penetration in the electric grid tends to tends to depress average wholesale grid electricity prices [62]. Consequently, we find that locations with low emissions intensity grid supply, synonymous with greater share of VRE generation, tend to also have lower LCOA. This explains why locations like West Texas, Oklahoma & Kansas with low CO_2 emission intensity grids tend to have

the lower LCOA compared to higher CO_2 intensity grid locations in Indiana and Illinois across all carbon policy scenarios (Figure 5-9). This observation also suggests that favored locations with lowest cost of ammonia production are likely to be robust to changes in carbon policy. An important caveat to this finding is the price-taker assumption implicit in our calculation that assumes the industrial process represents a relatively small electricity demand that and hence cannot influence electricity prices substantially.

5.4 The Role of Flexible Processes in exploring Cost Reduction Possibilities for Green Ammonia

As noted earlier, for dedicated VRE-based ammonia production, round-the-clock operation of the H-B synthesis loop requires continuous electricity supply that necessitates the need for deploying Li-ion battery storage. While grid electricity use can reduce the need for Li-ion battery storage and hence improve cost outcomes, it is likely to increase CO_2 emissions intensity of the ammonia produced. Here, we explore how innovations to introduce flexibility in the H-B synthesis loop operations can contribute towards lowering the cost of dedicated VRE-based ammonia production while still adhering to the same round-the-clock ammonia supply requirements. Specifically, we investigate the cost and design impacts of the following two modifications: a) allowing the H-B synthesis to function at outputs below its nameplate capacity while constraining its ramp rate (5% change from previous hourly production level) and b) allowing storage of produced ammonia to enable producing more than nameplate capacity at times of high VRE availability to make up for less than nameplate production at low VRE availability periods. We consider two forms of ammonia storage - large scale cryogenic ammonia storage at -33° C (larger than 20000 tonnes) and small scale high pressure storage systems (20 bar). The storage inclusion is modelled in the same methodology as the other storage modes in the system but the system is allowed to shutdown and dispatch the demand requirement from the on-site

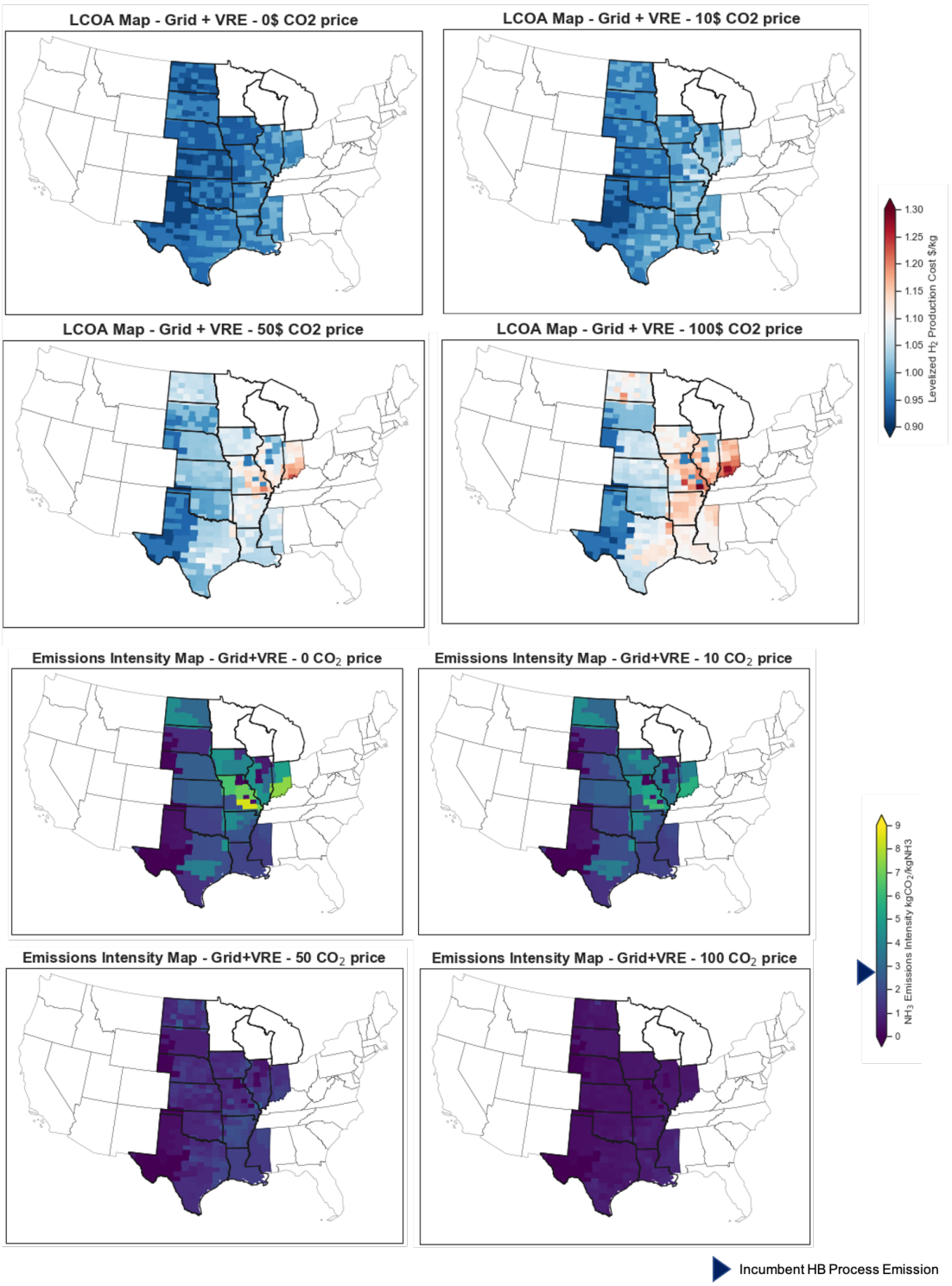

Figure 5-9: LCOA (top) and, (bottom) Average Emission Intensity Map for PV+wind Hybrid with Grid interconnection Electrolytic Ammonia production under different CO_2 scenarios

storage facility for ammonia. It should be noted that ammonia is still modeled to be output at a constant rate from the facility, which now includes ammonia storage and the H-B synthesis loop, since the produced ammonia might be used in other inflexible industrial processes (e.g. urea production). Figure 5-10 highlights that introducing the specified flexibility in the H-B synthesis loop (e.g. ability to turn down by 50 or 75% compared to nameplate and stay at that level for 48 hours) can enable a 5-10% decline in LCOA compared to the LCOA of the process where the H-B synthesis loop was inflexible. Figure 5-10 shows that the reduction in cost results from shifting the storage requirement downstream into the production process, with decreasing N_2 and H_2 storage and increasing NH_3 storage with increasing process flexibility. Moreover, the relative decrease in storage costs more than offsets the slight increase in cost of the H-B synthesis loop that needs to be oversized compared to the case of the inflexible process to enable NH_3 storage. In both the cases of flexible operations for the system we find that the outcomes Overall, this framework can be used to study the maximum affordable cost impacts of innovations to improve process flexibility that are valued in terms of improving the process economics.

5.5 Sensitivity Analysis to Capital Cost Projections

Our analysis shows that the impact of lowering renewable electricity costs can have a great impact on changing the effective levelized cost of producing Ammonia from Gen II HB systems. As we have shown in the previous sections, the cost stack of electrolytic H_2 driven Ammonia processes is dominated by VRE resource CAPEX. A decline in the costs of the same or variation can have impacts as high as 40% on the currently estimated 2030 cost scenario.(Figure 5-11).

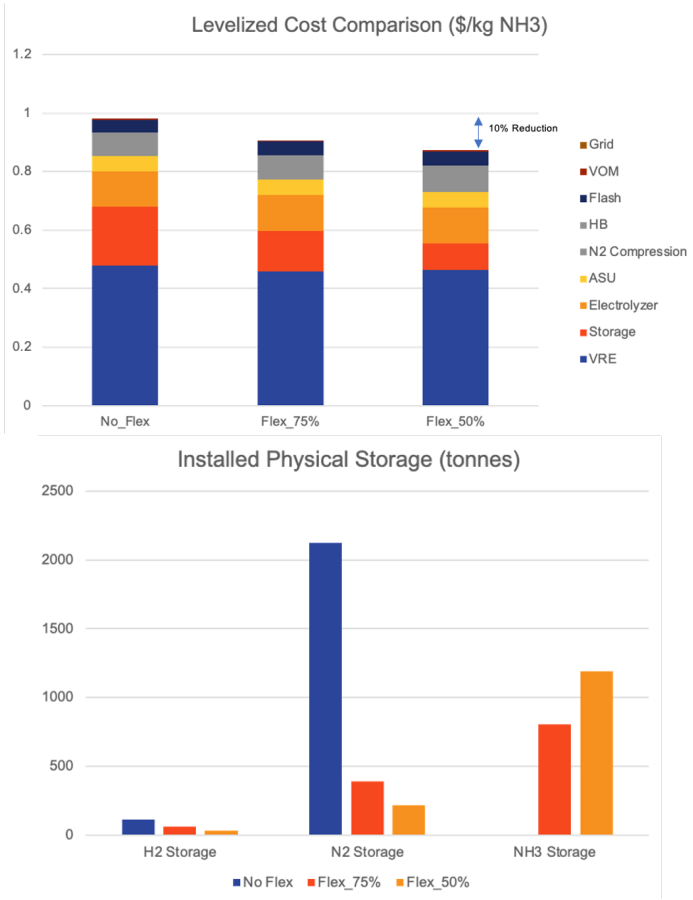

Figure 5-10: LCOA stack for flexible HB Systems in Ammonia synthesis for no flexibility, HB system turndown to 75 percent of design flow rate and system turndown to 50 percent of design flow rate (top), Storage Capacity Installed for Flexibility Cases (bottom)

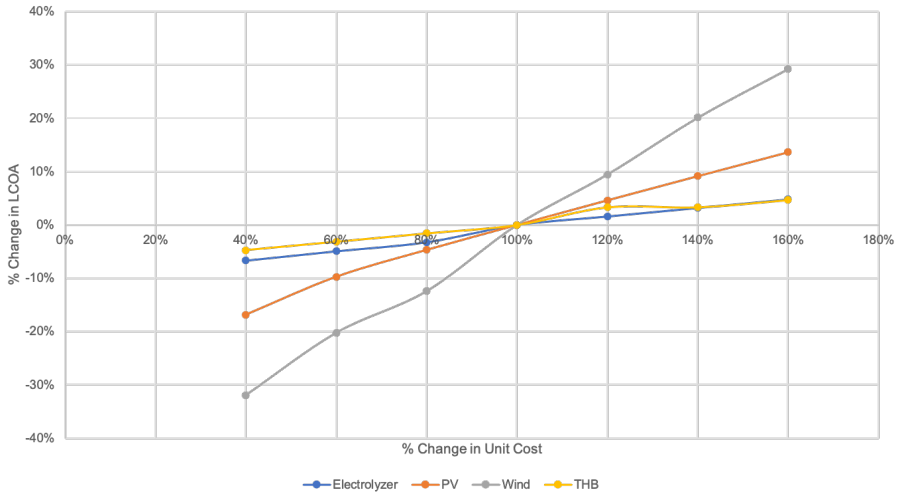

Figure 5-11: Impact of CAPEX variation for NH_3 synthesis process components

Chapter 6

Conclusions and Key Takeaways

Here, we propose a systematic framework to explore the economics and CO_2 emissions impacts of commercially available electricity-driven ammonia production schemes while considering spatial and temporal variations in electricity supply from the grid as well as on-site production via VRE resources. Our findings are based on a design and operations modeling framework that allows for co-optimizing the size of various components, including grid connection, electricity, H_2, and N_2 generation capacity and different types of on-site storage while enabling round-the-clock steady ammonia production. Based on 2030 technology cost and electric grid projections, we find that ammonia produced solely via grid electricity could achieve lower CO2 emissions intensity as compared to natural gas based ammonia in some locations (e.g. Texas) but could also lead to higher CO2 emissions intensity in other locations (E.g. Indiana). In Midcontental U.S. regions with existing agricultural ammonia demand, we estimate the LCOA of grid-based ammonia to be 0.5-0.6 \$/kg that corresponds to an abatement cost range of –35 \$/tonne CO_2 (higher emissions than natural gas based process) to 52 \$/tonne CO_2 (lower emissions than natural gas based process). In contrast to grid electricity use, dedicated wind and solar PV based ammonia production can reduce process CO_2 emissions by 100% but have widely different process designs and abatement costs depending on location, and configuration of VRE supply. Across the U.S. , we investigated the cost of VRE-based electricity driven ammonia production and estimated the 5th percentile, median and 95th percentile values for resulting CO2

abatement cost to be: 1) 314, 536, 936 $/tonne CO2 for PV –based electricity supply, 2) 373, 653, 1879 $/tonne CO2 for wind-based electricity supply and 3) 262, 334, 577 $/tonne CO2 for PV+Wind based electricity supply. The combination of grid +co-located VRE electricity supply locations may be the most cost-effective way for low-carbon grid based ammonia production since it reduces the on-site energy storage requirements for continuous ammonia production. In the midcontinent US states with existing agricultural ammonia demand, we find that 2030 grid +VRE connected ammonia under a $50/tonne CO2 policy scenario can achieve 60-90% CO2 emissions reduction per tonne of ammonia produced compared to natural gas based routes, which corresponds to an abatement cost of 21-184 $/tonne. Finally, a key driver for cost of dedicated VRE systems is the need for battery storage to enable continuous power supply for the H-B synthesis loop. In this context, enabling operational flexibility in H-B synthesis to allow some ramping capability in ammonia production could be beneficial in reducing the cost of VRE-based ammonia supply. This analysis also suggests that emerging ammonia production routes that use electrochemical rather than thermochemical synthesis schemes may be more synergistic and cost-effective for using VRE electricity input. The methodological contributions of this thesis in modeling the design and operation of electricity-driven chemical production can be extended to study other key industrial commodities with large carbon footprint like steel, cement, ethylene and methanol. Moreover, the developed framework can also be readily used to study industrial process decarbonization for other geographies, such as many developing countries which predominantly rely on coal for primary energy use. In these regions, the CO2 abatement cost of VRE electricity-based ammonia production is likely to be lower than values estimated in the U.S. context in this study. The findings of this study should be interpreted keeping in mind the following limitations, which also are interesting areas of future work. First, our assessment of process and grid interactions are based on a price taker assumption that assumes no change in wholesale electricity prices or marginal grid emissions factors due to increasing grid electricity consumption by the ammonia production process. An interesting area of future work would be to represent industrial demand with flexibility constraints in

grid operations models to understand the complete picture of large-scale electrification of industrial processes. Second, our spatial assessment of LCOA does not account for spatial variation in the cost of land or the cost of transporting ammonia from the production site to the point of consumption. Accounting for these attributes may lead to some locations being more favorable than others in terms of delivered cost of ammonia rather than LCOA metric used here. Third, our analysis relied on characterizing VRE resource availability based on a single weather year and while this is reasonable for a screening analysis, further assessment is needed to understand the impacts of inter-annual variability in VRE output as well as the impacts of climate change on VRE variability on LCOA of VRE-based ammonia production.

Appendix A

Appendix

A.1 Model Component Summary - ASPEN Simulation Results

Table A.1: Process Heater Summary

	Heater		
Name	**COOL3**	**COOL4**	**HEAT1**
Property method	**RKS-BM**	**RKS-BM**	**RKS-BM**
Use true species approach for electrolytes	**YES**	**YES**	**YES**
Free-water phase properties method	**STEAM-TA**	**STEAM-TA**	**STEAM-TA**
Water solubility method	**3**	**3**	**3**
Specified pressure [bar]	**0**	**0**	**100**
Specified temperature [C]	**50**	**50**	
EO Model components			
Calculated pressure [bar]	30	81	6.89
Calculated temperature [C]	50	50	164.83
Calculated vapor fraction	1	1	0.28
Calculated heat duty [cal/sec]	166905.85	-810640.14	8664171.02
Pressure-drop correlation parameter			
Net duty [cal/sec]	166905.85	-810640.14	0

Table A.2: Heat Exchanger

HeatX	
Name	**HEX**
Hot side property method	**RKS-BM**
Hot side Henry's component list ID	
Hot side electrolyte chemistry ID	
Hot side use true species approach for electrolytes	**YES**
Hot side free-water phase properties method	**STEAM-TA**
Hot side water solubility method	**3**
Cold side property method	**RKS-BM**
Cold side Henry's component list ID	
Cold side electrolyte chemistry ID	
Cold side use true species approach for electrolytes	**YES**
Cold side free-water phase properties method	**STEAM-TA**
Cold side water solubility method	**3**
Exchanger specification	**330**
Units of exchanger specification	**C**
Inlet hot stream temperature [C]	500
Inlet hot stream pressure [bar]	250
Inlet hot stream vapor fraction	1
Outlet hot stream temperature [C]	247.45
Outlet hot stream pressure [bar]	250
Outlet hot stream vapor fraction	1
Inlet cold stream temperature [C]	89.93
Inlet cold stream pressure [bar]	250
Inlet cold stream vapor fraction	1
Outlet cold stream temperature [C]	330
Outlet cold stream pressure [bar]	250
Outlet cold stream vapor fraction	1
Heat duty [cal/sec]	4133482.86
Calculated heat duty [cal/sec]	4133482.86
Required exchanger area [sqm]	124.38
Actual exchanger area [sqm]	124.38
Average U (Dirty) [cal/sec-sqcm-K]	0.02
Average U (Clean)	
UA [cal/sec-K]	25253.36
LMTD (Corrected) [C]	163.68
LMTD correction factor	1
Number of shells in series	1
Number of shells in parallel	

Table A.3: Flash Unit

Flash2	
Name	**FLASH2**
Property method	**RKS-BM**
Use true species approach for electrolytes	**YES**
Free-water phase properties method	**STEAM-TA**
Water solubility method	**3**
Temperature [C]	**-14.3**
Pressure [bar]	**170**
Specified vapor fraction	
Specified heat duty [cal/sec]	**0**
EO Model components	
Outlet temperature [C]	-14.3
Outlet pressure [bar]	170
Vapor fraction	0.80
Heat duty [cal/sec]	-5984076.36
Net duty [cal/sec]	-5984076.36
First liquid / total liquid	1

Table A.4: Reactor

RGibbs	
Name	**REACTOR**
Property method	**RKS-BM**
Henry's component list ID	
Electrolyte chemistry ID	
Use true species approach for electrolytes	**YES**
Free-water phase properties method	**STEAM-TA**
Water solubility method	**3**
Specified pressure [bar]	**250**
Specified temperature [C]	**500**
Specified heat duty [cal/sec]	**0**
EO Model components	
Outlet temperature [C]	500
Outlet pressure [bar]	250
Calculated heat duty [cal/sec]	-2036360.37
Net heat duty [cal/sec]	-2036360.37
Vapor fraction	1
Number of fluid phases	1

Table A.5: Compressor

	Compr				
Name	**B3**	**CMP3**	**CMP4**	**CMP5**	**RECCOMP1**
Property method	**RKS-BM**	**RKS-BM**	**RKS-BM**	**RKS-BM**	**RKS-BM**
Henry's component list ID					
Electrolyte chemistry ID					
Use true species approach for electrolytes	**YES**	**YES**	**YES**	**YES**	**YES**
Free-water phase properties method	**STEAM-TA**	**STEAM-TA**	**STEAM-TA**	**STEAM-TA**	**STEAM-TA**
Water solubility method	**3**	**3**	**3**	**3**	**3**
Model Type	**ASME-ISENTROP**	**ISENTROPIC**	**ASME-ISENTROP**	**ASME-ISENTROP**	**ASME-ISENTROP**
Specified discharge pressure [bar]	**1**	**30**	**81**	**250**	**250**
Isentropic efficiency	**0.7**				
Indicated horsepower [kW]	-2207.68	0	3413.33	4168.89	2221.25
Calculated brake horsepower [kW]	-2207.68	0	3413.33	4168.89	2221.25
Net work required [kW]	-2207.68	0	3413.33	4168.89	2221.25
Efficiency (polytropic / isentropic) used	0.7	0.72	0.72	0.72	0.72
Calculated discharge pressure [bar]	1	30	81	250	250
Calculated pressure change [bar]	5.89475729	0	51	169	80
Calculated pressure ratio	0.14	1	2.7	3.08	1.47
Outlet temperature [C]	102.08	19.14	197.67	222.40	28.48
Isentropic outlet temperature [C]	102.08	19.14	156.01	172.35	16.33
Vapor fraction	0.35	1	1	1	1
Head developed [m-kgf/kg]	-11577.66	0	37667.25	46005.07	10454.92
Isentropic power requirement [kW]	-3153.83	0	2457.60	3001.60	1599.30
Inlet heat capacity ratio	1.62	1	1.41	1.42	1.49
Inlet volumetric flow rate [l/min]	136533.64	38281.47	42312.78	16155.28	13489.84
Outlet volumetric flow rate [l/min]	1029185.12	38281.47	23320.01	8555.54	11220.87
Inlet compressibility factor	0.27		1.01	1.04	1.10
Outlet compressibility factor	0.35		1.039	1.11	1.15

A.2 Stream Summary - ASPEN Simulation Results

Table A.6: Stream Table - Part 1 of 2

Stream Name	**Units**	**AM**	**HN1**	**HN6**	**HN7**	**HN8**	**HN9**	**HN10**	**HYDROGEN**	**N-H-AM**	**NITROGEN**
Description											
From		MAINSEP	FEEDMIX	CMP3	COOL3	CMP4	COOL4	CMP5		MIX	
To			CMP3	COOL3	CMP4	COOL4	CMP5	MIX	FEEDMIX	PRG-SPT	FEEDMIX
Stream Class		CONVEN	CONVEN	CONVEN	CONVEN	CONVEN	CONVEN	CONVEN	CONVEN	CONVEN	CONVEN
Maximum Relative Error											
Cost Flow	$/hr										
MIXED Substream											
Phase		Liquid Phase	Vapor Phase	Vapor Phase	Vapor Phase	Vapor Phase	Vapor Phase	Vapor Phase	Vapor Phase	Vapor Phase	Vapor Phase
Temperature	C	-14.30	19.14	19.14	50.00	197.67	50.00	222.41	20.00	89.93	20.00
Pressure	bar	170.00	30.00	30.00	30.00	81.00	81.00	250.00	30.00	250.00	30.00
Molar Vapor Fraction		0.00	1.00	1.00	1.00	1.00	1.00	1.00	1.00	1.00	1.00
Molar Liquid Fraction		1.00	0.00	0.00	0.00	0.00	0.00	0.00	0.00	0.00	0.00
Molar Solid Fraction		0.00	0.00	0.00	0.00	0.00	0.00	0.00	0.00	0.00	0.00
Mass Vapor Fraction		0.00	1.00	1.00	1.00	1.00	1.00	1.00	1.00	1.00	1.00
Mass Liquid Fraction		1.00	0.00	0.00	0.00	0.00	0.00	0.00	0.00	0.00	0.00
Mass Solid Fraction		0.00	0.00	0.00	0.00	0.00	0.00	0.00	0.00	0.00	0.00
Molar Enthalpy	cal/mol	-16614.68	-40.80	-40.80	174.92	1228.60	180.89	1467.81	-28.34	301.21	-77.78
Mass Enthalpy	cal/gm	-972.14	-4.74	-4.74	20.34	142.88	21.04	170.70	-14.06	32.26	-2.76
Molar Entropy	cal/mol-K	-47.74	-5.75	-5.75	-5.05	-4.39	-7.07	-6.30	-6.86	-8.71	-6.89
Mass Entropy	cal/gm-K	-2.79	-0.67	-0.67	-0.59	-0.51	-0.82	-0.73	-3.40	-0.93	-0.24
Molar Density	mol/cc	0.03	0.00	0.00	0.00	0.00	0.00	0.01	0.00	0.01	0.00
Mass Density	gm/cc	0.53	0.01	0.01	0.01	0.02	0.02	0.05	0.00	0.07	0.03
Enthalpy Flow	cal/sec	-6357856.96	-31567.61	-31567.61	135338.24	950600.32	139960.18	1135684.25	-16397.77	717713.39	-15169.84
Average MW		17.09	8.60	8.60	8.60	8.60	8.60	8.60	2.02	9.34	28.13
Mole Flows	kmol/hr	1377.59	2785.42	2785.42	2785.42	2785.42	2785.42	2785.42	2083.33	8577.97	702.08
H2	kmol/hr	5.55	2083.33	2083.33	2083.33	2083.33	2083.33	2083.33	2083.33	6162.93	0.00
N2	kmol/hr	1.99	695.06	695.06	695.06	695.06	695.06	695.06	0.00	2119.99	695.06
NH3	kmol/hr	1363.75	0.00	0.00	0.00	0.00	0.00	0.00	0.00	152.53	0.00
AR	kmol/hr	6.31	7.02	7.02	7.02	7.02	7.02	7.02	0.00	142.51	7.02
CW	kmol/hr	0.00	0.00	0.00	0.00	0.00	0.00	0.00	0.00	0.00	0.00
Mole Fractions											
H2		0.00	0.75	0.75	0.75	0.75	0.75	0.75	1.00	0.72	0.00
N2		0.00	0.25	0.25	0.25	0.25	0.25	0.25	0.00	0.25	0.99
NH3		0.99	0.00	0.00	0.00	0.00	0.00	0.00	0.00	0.02	0.00
AR		0.00	0.00	0.00	0.00	0.00	0.00	0.00	0.00	0.02	0.01
CW		0.00	0.00	0.00	0.00	0.00	0.00	0.00	0.00	0.00	0.00

Table A.7: Stream Table - Part 2 of 2

Stream Name	**Units**	**PURGE**	**REC**	**REMAIN**	**RXN-CLD**	**RXN-FEED**	**RXN-PROD**	**S1**	**S6**	**S15**	**S16**
Description											
From		PRG-SPT	MAINSEP	PRG-SPT	HEX	HEX	REACTOR	RECCOMP1	B3		HEAT1
To			RECCOMP	HEX	MAINSEP	REACTOR	HEX	MIX		HEAT1	B3
Stream Class		CONVEN	CONVEN	CONVEN	CONVEN	CONVEN	CONVEN	CONVEN	CONVEN	CONVEN	CONVEN
Maximum Relative Error											
Cost Flow	$/hr										
MIXED Substream											
Phase		Vapor Phase	Vapor Phase	Vapor Phase	Vapor Phase	Vapor Phase	Vapor Phase	Vapor Phase		Liquid Phase	
Temperature	C	89.93	-14.30	89.93	247.45	330.00	500.00	28.49	102.08	25.00	164.83
Pressure	bar	250.00	170.00	250.00	250.00	250.00	250.00	250.00	1.00	1.00	6.89
Molar Vapor Fraction		1.00	1.00	1.00	1.00	1.00	1.00	1.00	0.36	0.00	0.29
Molar Liquid Fraction		0.00	0.00	0.00	0.00	0.00	0.00	0.00	0.64	1.00	0.71
Molar Solid Fraction		0.00	0.00	0.00	0.00	0.00	0.00	0.00	0.00	0.00	0.00
Mass Vapor Fraction		1.00	1.00	1.00	1.00	1.00	1.00	1.00	0.36	0.00	0.29
Mass Liquid Fraction		0.00	0.00	0.00	0.00	0.00	0.00	0.00	0.64	1.00	0.71
Mass Solid Fraction		0.00	0.00	0.00	0.00	0.00	0.00	0.00	0.00	0.00	0.00
Molar Enthalpy	cal/mol	301.21	-589.48	301.21	-663.89	2044.67	1411.40	-259.76	-63716.24	-68993.41	-63374.26
Mass Enthalpy	cal/gm	32.26	-60.81	32.26	-59.73	218.96	126.98	-26.80	-3536.79	-3829.72	-3517.81
Molar Entropy	cal/mol-K	-8.71	-10.52	-8.71	-9.90	-5.02	-6.65	-10.21	-26.25	-40.82	-26.64
Mass Entropy	cal/gm-K	-0.93	-1.09	-0.93	-0.89	-0.54	-0.60	-1.05	-1.46	-2.27	-1.48
Molar Density	mol/cc	0.01	0.01	0.01	0.01	0.00	0.00	0.01	0.00	0.04	0.00
Mass Density	gm/cc	0.07	0.07	0.07	0.06	0.04	0.04	0.08	0.00	0.76	0.01
Enthalpy Flow	cal/sec	3588.57	-948530.97	714124.82	-1322311.58	4847607.68	2811171.28	-417970.87	-98244129.16	-106381003.63	-97716832.61
Average MW		9.34	9.69	9.34	11.12	9.34	11.12	9.69	18.02	18.02	18.02
Mole Flows	kmol/hr	42.89	5792.74	8535.08	7170.33	8535.08	7170.33	5792.55	5550.84	5550.84	5550.84
H2	kmol/hr	30.81	4079.64	6132.12	4085.19	6132.12	4085.19	4079.60	0.00	0.00	0.00
N2	kmol/hr	10.60	1425.07	2109.39	1427.07	2109.39	1427.07	1424.93	0.00	0.00	0.00
NH3	kmol/hr	0.76	152.54	151.77	1516.29	151.77	1516.29	152.53	0.00	0.00	0.00
AR	kmol/hr	0.71	135.48	141.79	141.79	141.79	141.79	135.49	0.00	0.00	0.00
CW	kmol/hr	0.00	0.00	0.00	0.00	0.00	0.00	0.00	5550.84	5550.84	5550.84
Mole Fractions											
H2		0.72	0.70	0.72	0.57	0.72	0.57	0.70	0.00	0.00	0.00
N2		0.25	0.25	0.25	0.20	0.25	0.20	0.25	0.00	0.00	0.00
NH3		0.02	0.03	0.02	0.21	0.02	0.21	0.03	0.00	0.00	0.00
AR		0.02	0.02	0.02	0.02	0.02	0.02	0.02	0.00	0.00	0.00
CW		0.00	0.00	0.00	0.00	0.00	0.00	0.00	1.00	1.00	1.00

Bibliography

[1] "Sector share of ammonia emissions — european environment agency."

[2] "Ammonia—a renewable fuel made from sun, air, and water—could power the globe without carbon | science | AAAS."

[3] O. US EPA, "GHGRP non-fluorinated chemicals."

[4] D. B. Belzer, K. A. Cort, and S. Ganguli, "A comprehensive system of energy intensity indicators for the u.s.: Methods, data and key trends,"

[5] J. R. Bartels, *A feasibility study of implementing an Ammonia Economy*. Master of Science, Iowa State University, Digital Repository, Ames, 2008. Pages: 2807317.

[6] G. Chehade and I. Dincer, "Progress in green ammonia production as potential carbon-free fuel," vol. 299, p. 120845.

[7] M. Xue, Q. Wang, B.-L. Lin, and K. Tsunemi, "Assessment of ammonia as an energy carrier from the perspective of carbon and nitrogen footprints," vol. 7, no. 14, pp. 12494–12500. Publisher: American Chemical Society.

[8] IEA, "The future of hydrogen," *IEA*, 2019.

[9] "Fertilizer price increases for 2021 production • farmdoc daily."

[10] "India's ammonia capacity is expected to witness double digit growth over the next six years, says GlobalData." Section: Press Release.

[11] "Ammonia and urea cash cost | yara international."

[12] G. Inc, "Fertilizer use in africa: A price issue."

[13] "Yara plans green ammonia production in norway."

[14] "CF plans green ammonia plant in louisiana."

[15] "Green ammonia in australia, spain, and the united states."

[16] "Saudi arabia to export renewable energy using green ammonia."

[17] D. R. MacFarlane, P. V. Cherepanov, J. Choi, B. H. R. Suryanto, R. Y. Hodgetts, J. M. Bakker, F. M. F. Vallana, and A. N. Simonov, "A Roadmap to the Ammonia Economy," *Joule*, vol. 4, pp. 1186–1205, June 2020. Publisher: Elsevier.

[18] M. Wang, M. A. Khan, I. Mohsin, J. Wicks, A. H. Ip, K. Z. Sumon, C.-T. Dinh, E. H. Sargent, I. D. Gates, and M. G. Kibria, "Can sustainable ammonia synthesis pathways compete with fossil-fuel based Haber–Bosch processes?," *Energy & Environmental Science*, vol. 14, pp. 2535–2548, May 2021. Publisher: The Royal Society of Chemistry.

[19] N. Salmon and R. Bañares-Alcántara, "Green ammonia as a spatial energy vector: a review," *Sustainable Energy & Fuels*, vol. 5, no. 11, pp. 2814–2839, 2021. Publisher: Royal Society of Chemistry.

[20] B. M. Comer, P. Fuentes, C. O. Dimkpa, Y.-H. Liu, C. A. Fernandez, P. Arora, M. Realff, U. Singh, M. C. Hatzell, and A. J. Medford, "Prospects and Challenges for Solar Fertilizers," *Joule*, vol. 3, pp. 1578–1605, July 2019.

[21] B. M. Comer, P. Fuentes, C. O. Dimkpa, Y.-H. Liu, C. A. Fernandez, P. Arora, M. Realff, U. Singh, M. C. Hatzell, and A. J. Medford, "Prospects and Challenges for Solar Fertilizers," *Joule*, vol. 3, pp. 1578–1605, July 2019.

[22] V. Dias, M. Pochet, F. Contino, and H. Jeanmart, "Energy and Economic Costs of Chemical Storage," *Frontiers in Mechanical Engineering*, vol. 6, 2020. Publisher: Frontiers.

[23] O. Osman, S. Sgouridis, and A. Sleptchenko, "Scaling the production of renewable ammonia: A techno-economic optimization applied in regions with high insolation," *Journal of Cleaner Production*, vol. 271, p. 121627, Oct. 2020.

[24] M. M. Maia 1981, "Techno-economic analysis of green ammonia production using offshore wind farms." Accepted: 2021-06-24T09:50:26Z.

[25] S. A. Nosherwani and R. C. Neto, "Techno-economic assessment of commercial ammonia synthesis methods in coastal areas of germany," vol. 34, p. 102201.

[26] C. Fúnez Guerra, L. Reyes-Bozo, E. Vyhmeister, M. Jaén Caparrós, J. L. Salazar, and C. Clemente-Jul, "Technical-economic analysis for a green ammonia production plant in chile and its subsequent transport to japan," vol. 157, pp. 404–414.

[27] J. Li, J. Lin, P. M. Heuser, H. U. Heinrichs, J. Xiao, F. Liu, M. Robinius, Y. Song, and D. Stolten, "Co-planning of regional wind resources-based ammonia industry and the electric network: A case study of inner mongolia," pp. 1–1. Conference Name: IEEE Transactions on Power Systems.

[28] N. D. Pawar, H. U. Heinrichs, C. Winkler, P.-M. Heuser, S. D. Ryberg, M. Robinius, and D. Stolten, "Potential of green ammonia production in india,"

[29] R. Nayak-Luke, R. Bañares-Alcántara, and I. Wilkinson, ""Green" Ammonia: Impact of Renewable Energy Intermittency on Plant Sizing and Levelized Cost of Ammonia," *Industrial & Engineering Chemistry Research*, vol. 57, pp. 14607–14616, Oct. 2018. Publisher: American Chemical Society.

[30] F. I. Gallardo, A. Monforti Ferrario, M. Lamagna, E. Bocci, D. Astiaso Garcia, and T. E. Baeza-Jeria, "A techno-economic analysis of solar hydrogen production by electrolysis in the north of chile and the case of exportation from atacama desert to japan," vol. 46, no. 26, pp. 13709–13728.

[31] C. Liang, "Green haber-bosch process:a small-scale ammonia reactor system design,"

[32] O. Osman, S. Sgouridis, and A. Sleptchenko, "Scaling the production of renewable ammonia: A techno-economic optimization applied in regions with high insolation," *Journal of Cleaner Production*, vol. 271, p. 121627, Oct. 2020.

[33] R. Michael Nayak-Luke and R. Bañares-Alcántara, "Techno-economic viability of islanded green ammonia as a carbon-free energy vector and as a substitute for conventional production," vol. 13, no. 9, pp. 2957–2966. Publisher: Royal Society of Chemistry.

[34] E. R. Morgan, J. F. Manwell, and J. G. McGowan, "Sustainable ammonia production from u.s. offshore wind farms: A techno-economic review," vol. 5, no. 11, pp. 9554–9567.

[35] H. Zhang and U. Desideri, "TECHNO-ECONOMIC EVALUATION OF POWER-TO-AMMONIA SYSTEM," p. 4.

[36] R. Bañares-Alcántara, G. D. Iii, M. Fiaschetti, P. Grünewald, J. M. Lopez, E. Tsang, A. Yang, L. Ye, and S. Zhao, "Analysis of Islanded Ammonia-based Energy Storage Systems," p. 158.

[37] J. Armijo and C. Philibert, "Flexible production of green hydrogen and ammonia from variable solar and wind energy: Case study of chile and argentina," vol. 45, no. 3, pp. 1541–1558.

[38] S. Schulte Beerbühl, M. Fröhling, and F. Schultmann, "Combined scheduling and capacity planning of electricity-based ammonia production to integrate renewable energies," *European Journal of Operational Research*, vol. 241, pp. 851–862, Mar. 2015.

[39] A. Allman and P. Daoutidis, "Optimal scheduling for wind-powered ammonia generation: Effects of key design parameters," *Chemical Engineering Research and Design*, vol. 131, pp. 5–15, Mar. 2018.

[40] H. Zhang, L. Wang, J. Van herle, F. Maréchal, and U. Desideri, "Techno-economic comparison of green ammonia production processes," *Applied Energy*, vol. 259, no. C, 2020. Publisher: Elsevier.

[41] D. S. Mallapragada, E. Gençer, P. Insinger, D. W. Keith, and F. M. O'Sullivan, "Can Industrial-Scale Solar Hydrogen Supplied from Commodity Technologies Be Cost Competitive by 2030?," *Cell Reports Physical Science*, p. 100174, Aug. 2020.

[42] Gurobi Optimization, LLC, "Gurobi Optimizer Reference Manual," 2021.

[43] A. Reuther, J. Kepner, C. Byun, S. Samsi, W. Arcand, D. Bestor, B. Bergeron, V. Gadepally, M. Houle, M. Hubbell, M. Jones, A. Klein, L. Milechin, J. Mullen, A. Prout, A. Rosa, C. Yee, and P. Michaleas, "Interactive supercomputing on 40,000 cores for machine learning and data analysis," in *2018 IEEE High Performance extreme Computing Conference (HPEC)*, pp. 1–6, IEEE, 2018.

[44] "Hydrogen Delivery Infrastructure Analysis."

[45] S. Akar, P. Beiter, W. Cole, D. Feldman, P. Kurup, E. Lantz, R. Margolis, D. Oladosu, T. Stehly, G. Rhodes, C. Turchi, and L. Vimmerstedt, "2020 annual technology baseline (atb) cost and performance data for electricity generation technologies,"

[46] R. Ahluwalia, "System Level Analysis of Hydrogen Storage Options," p. 42.

[47] J. Kim, Y. Noh, and D. Chang, "Storage system for distributed-energy generation using liquid air combined with liquefied natural gas," vol. 212, pp. 1417–1432.

[48] "Storage and shipping," in *Ammonia*, pp. 213–220, John Wiley & Sons, Ltd. Section: 9 _eprint: https://onlinelibrary.wiley.com/doi/pdf/10.1002/9783527613885.ch09.

[49] Linde, "Nitrogen Generation by Pressure Swing Adsorption," 2021.

[50] C. D. Demirhan, W. W. Tso, J. B. Powell, and E. N. Pistikopoulos, "A multi-scale energy systems engineering approach towards integrated multi-product network optimization," vol. 281, p. 116020.

[51] P. R. Brown and A. Botterud, "The value of inter-regional coordination and transmission in decarbonizing the US electricity system," vol. 5, no. 1, pp. 115–134.

[52] M. Sengupta, Y. Xie, A. Lopez, A. Habte, G. Maclaurin, and J. Shelby, "The national solar radiation data base (NSRDB)," vol. 89, pp. 51–60.

[53] W. F. Holmgren, C. W. Hansen, and M. A. Mikofski, "pvlib python: a python package for modeling solar energy systems," vol. 3, no. 29, p. 884.

[54] A. Dobos, "PVWatts version 5 manual."

[55] C. Draxl, B. M. Hodge, A. Clifton, and J. McCaa, "Overview and meteorological validation of the wind integration national dataset toolkit."

[56] C. Draxl, A. Clifton, B.-M. Hodge, and J. McCaa, "The wind integration national dataset (WIND) toolkit," vol. 151, pp. 355–366.

[57] W. Lieberman-Cribbin and C. University, "A guide to using the WIND toolkit validation code," p. 31.

[58] J. King, A. Clifton, and B. Hodge, "Validation of power output for the WIND toolkit."

[59] W. Cole, S. Corcoran, N. Gates, T. Mai, and P. Das, "2020 standard scenarios report: A u.s. electricity sector outlook," p. 51.

[60] M. P. S. Thind, E. J. Wilson, I. L. Azevedo, and J. D. Marshall, "Marginal emissions factors for electricity generation in the midcontinent ISO," vol. 51, no. 24, pp. 14445–14452.

[61] "Price gouging or price reality? anhydrous ammonia prices climb 60% since fall."

[62] J. Seel, A. D. Mills, R. H. Wiser, S. Deb, A. Asokkumar, M. Hassanzadeh, and A. Aarabali, "Impacts of high variable renewable energy futures on wholesale electricity prices, and on electric-sector decision making."